Parcellation of Prefrontal Cortical Areas in Mouse and Rat Brain

van de Werd, H.J.J.M.

2013

document version
Publisher's PDF, also known as Version of record

Chapter 4

Comparison of (stereotactic) parcellations in mouse prefrontal cortex

With Harry B.M. Uylings
submitted for publication

Abstract

This study compares the cytoarchitectonic parcellation of the prefrontal cortex (PFC) in the mouse as presented in publications that are most commonly used for identifying brain areas. Agreement was found to be greater for boundaries in the medial PFC, than in the lateral PFC and least for those in the orbital areas of the PFC. In this review we explain and illustrate in a selected series of photographs and stereotactic pictures the differences in location and terminology of the different prefrontal cortical areas. The significance of cytoarchitectonic parcellation is discussed.

Keywords Cytoarchitecture - Stereotactic atlas - mouse strain - C57BL/6

Abbreviations

ACd	Dorsal anterior cingulate cortex
ACv	Ventral agranular cingulate area
ACvd	Ventral agranular cingulate area, dorsal part
ACvv	Ventral agranular cingulate area, ventral part
AId_1	Dorsal agranular insular area, dorsal part
AId_2	Dorsal agranular insular area, ventral part
AIp	Posterior agranular insular area
cc	corpus callosum
DI	Dysgranular insular area
DLO	Dorsolateral orbital area
Fr1	Frontal area 1
Fr 2	Frontal area 2
G	Granular cortex
GI	Granular insular area
IG	Indusium griseum
IL	Infralimbic area
LO	Lateral orbital area
MO	Medial orbital area
PFC	Prefrontal cortex
PL	Prelimbic area
PLd	Prelimbic area, dorsal part
PLv	Prelimbic area, ventral part
RSA	Agranular retrosplenial cortex
RSG	Granular retrosplenial cortex
VLO	Ventrolateral orbital area
VLOp	Posterior ventrolateral orbital area
VO	Ventral orbital area

Contents

1. Introduction

In our study of the rat prefrontal cortex (PFC) (Van de Werd and Uylings, 2008) and of the mouse PFC (Van de Werd et al., 2010), we defined boundaries of PFC areas on the basis of specified changes in the cytoarchitecture. For validation, we compared the boundaries assessed in the Nissl staining with boundaries visible in a number of histocytochemical stainings. Considerable variations are found in the parcellation of the prefrontal cortex (PFC) of the mouse shown in Nissl stained coronal sections by different authors. Our aim is to analyze the differences and to discuss the possible causes. In this review we compare the parcellations of the PFC as shown in the cytoarchitectonic/ stereotactic atlases of Franklin and Paxinos (2008) and Hof et al. (2000), the cytoarchitectonic atlas of Rose (1929) and the studies of Caviness (1975) and Wree et al. (1983) with our study (Van De Werd et al. 2010) as well as with each other. In a selected series of photographs and stereotactic pictures of the original figures we have also displayed the 'Van de Werd et al.' PFC boundaries. In this way the differences between the original parcellations are made directly visible.

Cytoarchitectonic features of the mouse cerebral cortical areas, including individual frontal areas, have been described in the atlas of Rose (1929) and in the papers of De Vries (1912), Tsuneda (1937) and Caviness (1975). It is common, that in stereotactic atlases features for cortical boundaries are not explicitly described.

2. Materials and Methods

2.1. Material

Pairs of 'Nissl' photographs and their corresponding stereotactic drawings, which contain the PFC, were studied from the mouse cytoarchitectonic/ stereotactic atlases of Franklin and Paxinos (2008; strain C57BL/6) and Hof et al. (2000; strain C57BL/6). From Rose (1929; strain unspecified) and Cavines (1975; hybrid mice C3Hx-C57BL/6J) 'Nissl' photographs and

from Wree et al. (1983; strain BULB/c) pairs of 'Nissl' photographs and the accompanying Grey Level Index (GLI) pictures have been analyzed from the frontal region. The selected photographs and stereotactic schemes represent coronal sections from the anterior part of the PFC to the beginning of the retrosplenial region. In general, cytoarchitectonic delineation characteristics are sufficiently visible in these original Nissl photographs to allow a comparison of the original parcellations with our parcellation (Van de Werd et al. 2010; strain C57BL/6).

The original Nissl-photographs and stereotactic drawings were transferred into Corel Draw 12 to insert the cortical boundaries of the prefrontal areas based upon our criteria. After the completion of these drawings, the Corel Draw files were converted into PDF files and TIFF files to provide the figures for this paper.

2.2. Cytoarchitectonic criteria and nomenclature

Our approach in cytoarchitectonic parcellation is the characterization of the cytoarchitectonic features of the boundaries between cortical areas (Van Eden and Uylings 1985; Uylings and Van Eden 1990; Van de Werd et al. 2010; Uylings et al 2010). A condition for the characterization of boundaries is that their description can be applied by other students for reproducible delineation. We prefer such an approach to the mere characterization of the areas as a whole, which is the general practice of cytoarchitectonic descriptions. The cytoarchitectonic criteria used in this study were published in earlier papers (Van de Werd and Uylings 2008; Van de Werd et al. 2010). These cytoarchitectonic criteria were based on the following criteria: (a) granularity of layer IV, (b) presence and direction of curvilinear columns/rows of cell somata through the layers, (c) visibility of separate (sub)layers, (d) cell density and relative soma sizes in the different cortical layers, (e) dispersion or clustering of somata in layers, and (f) absolute and relative thickness of cortical layers and (g) relative position of cortical layers.

In Appendix 1, these characteristics have been summarized. The stereotactic levels are presented by the distance from the Bregma as indicated in the atlas of origin, i.e., the Franklin and Paxinos atlas (2008) for Figs. 1-10, and the Hof et al. atlas (2000) for figs.11-19.

The nomenclature for mouse PFC areas is based on Ray and Price (1992), adapted by Uylings and Van Eden (1990) and Van de Werd et al. (2010).

3. Results

In the descriptions that follow we have used bold writing to indicate the 'Van de Werd et al' nomenclature, italics to indicate the nomenclature of the authors of the atlases. In the photographs we have used regular letters to indicate our abbreviations. The stereotactic atlas of Franklin and Paxinos (2008) offers the access to high resolution plates. The atlas of Hof et al., 2000) offers 300 DPI resolution plates on CD-roms.

3.1. Comparison with Franklin and Paxinos (2008)

General remarks

On the lateral side of the frontal lobe, in contrast with the atlas of Franklin and Paxinos (2008), we have chosen to draw the boundaries up to the white matter. As a consequence the claustrum is included in our parcellation of the lateral PFC although it is strictly not part of the PFC.

3.1.1. Frontal pole

Bregma 2.80 mm (Fig.1): The lateral boundary of the frontal area 2, **Fr2**, is approximately equal to the boundary between the *prelimbic area* and the *frontal association cortex* (*PrL/FRA).* **Fr2** is equal to the dorsolateral part of the *prelimbic area* (*PrL). PrL* corresponds to the very high activity of acetylcholinesterase in layer III, rather than to the characteristics visible in the Nissl stain. At this level *Prl* encompasses, in addition to area **Fr2,** the dorsal anterior cingulate area (**ACd**) and the dorsal part of the prelimbic area (**PLd**), see Appendix 1 for differentiating cytoarchitectonic characteristics.

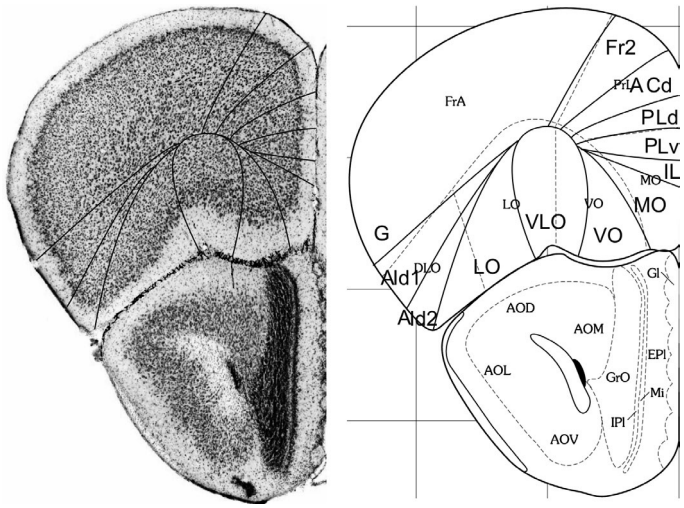

Fig. 1 Implementation of 'Van de Werd et al., 2010' boundaries at Bregma 2.80 mm. *(adapted from Franklin & Paxinos, 2008, The Mouse Brain in Stereotactic Coordinates, Academic Press, Elsevier, N.Y., USA).*

In the ventral part of the medial PFC, which encompasses the ventral prelimbic area (**PLv**), the infralimbic area (**IL**) and the medial orbital area (**MO**), the general density of cell-packing is higher than in the dorsal part of the medial PFC. These three areas offer a more detailed parcellation of the ventral part of the medial PFC than shown in the atlas, in which the whole ventral part of the medial PFC consists of only the *medial orbital area (MO).* On the lateral side of the frontal lobe in Franklin and Paxinos (2008), the dorsolateral orbital area *DLO* is specified as a more or less quadrangular field along the ventro-lateral side of the frontal lobe (Figs. 1, 2). In the parcellation of Van de Werd et al. (2010), only the dorsal agranular insular areas **AId1** and **AId2** are present as areas of the lateral PFC. In the mouse Van de Werd et al. (2010) did not find the characteristic cytoarchitecture of area **DLO** as defined in the rat (Van de Werd and Uylings, 2008). The cytoarchitecture of **AId1** and **AId2** in Fig. 1 is not different from the cytoarchitecture of the areas located more posteriorly. At this level, **AId1** is located ventrally to the granular cortex, **G**. The parcellation on the ventral/orbital side of the frontal lobe will be discussed in the evaluation of the next figure, Fig. 2.

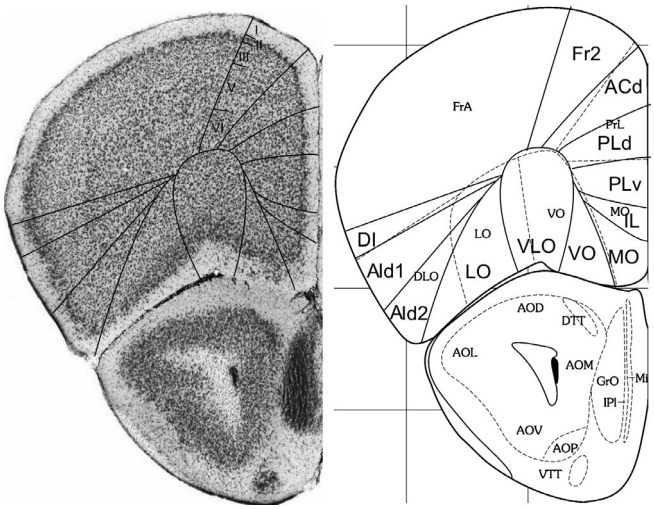

Fig. 2 Implementation of 'Van de Werd et al., 2010' boundaries at Bregma 2.58 mm. *(adapted from Franklin & Paxinos, 2008, The Mouse Brain in Stereotactic Coordinates, Academic Press, Elsevier, N.Y., USA).*

Bregma 2.58 mm (Fig. 2): The characteristics of the boundaries in the medial PFC are more clearly visible than they were in Fig. 1. At this level **Fr2** is no longer included in *PrL*, but is now located in *FrA.* This is due to the change of the dorsal boundary of *PrL* into a more medial position at this level. *PrL*, therefore, here includes a large part of **ACd** and **PLd.** On the lateral side of the frontal lobe the dysgranular insular area (**DI**) becomes visible between the ventral end of the band of layer IV granular cells that characterize the granular cortex and the dorsal agranular insular area, dorsal part, (**AId1**). Here the curvilinear arrangement of cells in the dorsal agranular insular areas **AId1** and **AId2** is better visible than in the previous Figure, as is also the difference in the density of packing of the cellular columns in these areas. On the ventral/orbital side of the frontal lobe, Van de Werd et al. (2010) distinguish the areas **VO**, **VLO** and **LO** (see Appendix 1), whereas no **VLO** is defined in the atlas, so that *ventral orbital area (VO)* encompasses the cytoarchitectonically different areas **VO** and a large part of **VLO** (see Appendix 1).

3.1.2. Frontal lobe anterior to the forceps minor

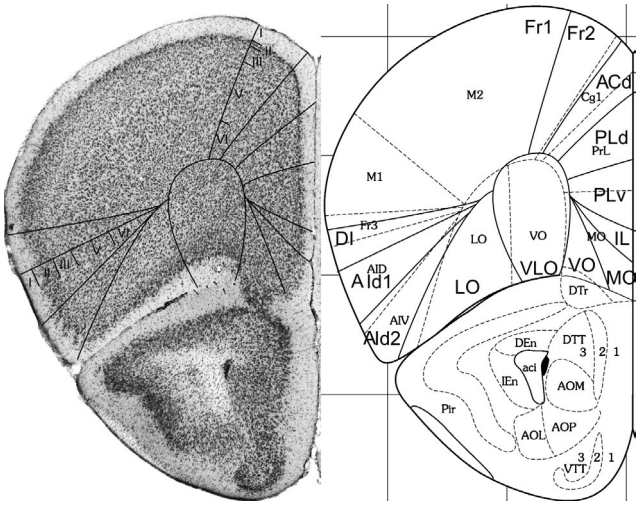

Fig. 3 Implementation of 'Van de Werd et al., 2010' boundaries at Bregma 2.34 mm. *(adapted from Franklin & Paxinos, 2008, The Mouse Brain in Stereotactic Coordinates, Academic Press, Elsevier, N.Y., USA).* **Fr1** : frontal area 1.

Bregma 2.34 mm (Fig.3): At this level area **Fr2** corresponds to the medial part of the *secondary motor area* (*M2*) and this correspondence remains visible in all the posterior sections of the PFC. The *cingulate area 1, Cg1,* is now indicated in the atlas, which is approximately in the same location as **ACd**. *PrL* encompasses **PLd**, and a dorsal part of **PLv**.

The location of area **VO**, which is different from the *ventral orbital area (VO)*, contacts now the retrobulbar region, i.e. the region behind the olfactory bulb encompassing the anterior olfactory nucleus. The atlas lacks a **VLO** area.

In the lateral PFC, the atlas defines a *ventral agranular insular area, AIV*, at this level, which roughly corresponds to **AId2.** Van Eden and Uylings (1985), Ray and Price (1992), and Van de Werd and Uylings (2008) defined in the rat an **AIv** as an area in the dorsal bank of the rhinal fissure. In the mouse, however, the **AIv** characteristics are not clearly found, so that they are not specified in the mouse sections. The *dorsal agranular insular area, AID,* is somewhat larger than **AId1.**

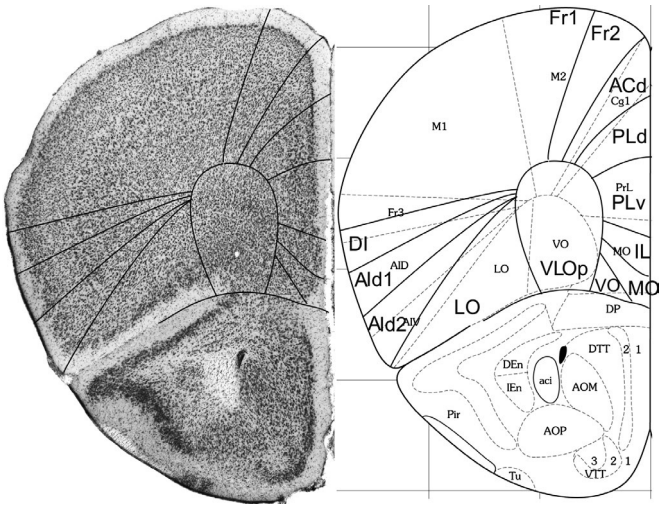

Fig. 4 Implementation of 'Van de Werd et al., 2010' boundaries at Bregma 2.10 mm. *(adapted from Franklin & Paxinos, 2008, The Mouse Brain in Stereotactic Coordinates, Academic Press, Elsevier, N.Y., USA).*

Bregma 2.10 mm (Fig. 4): The features of the areas in the medial PFC are as in the previous figures. The cortical layers in the posterior part of **VLO**, labelled **VLOp**, are more homogeneous with each other than they are in the anterior **VLO. VLOp** encompasses *VO* at this level. The granular cells in **DI** are sparse and difficult to distinguish. The areas **AId1** and **AId2** correspond roughly to respectively the areas *AID* and *AIV* in the atlas. In the lateral PFC, the differences between the Van de Werd et al. (2010) boundaries and the Franklin & Paxinos (2008) boundaries are explained by the gradual change of all characteristics at the respective boundaries.

3.1.3. Frontal lobe anterior to the genu of the corpus callosum

Bregma 1.94 mm (Fig. 5): The areas of the medial PFC are well distinguishable by the cytoarchitectonic differences in layer II, the cellular columns in the areas **Fr2** and **ACd**, and the arrangement of cells in the layer VI in rows, parallel to the cortical surface, in the areas **PLd**, **PLv**, **IL** and **MO** (see Appendix 1). *PrL* is approximately in the same location as **PLd** and **PLv**.

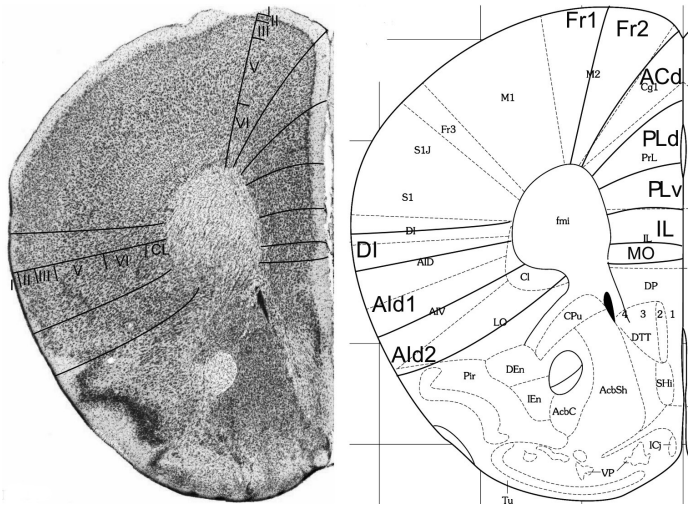

Fig. 5 Implementation of 'Van de Werd et al., 2010' boundaries at Bregma 1.94 mm. *(adapted from Franklin & Paxinos, 2008, The Mouse Brain in Stereotactic Coordinates, Academic Press, Elsevier, N.Y., USA)*

On the lateral side of the frontal lobe the prefrontal cortical layers can be followed as far as the piriform cortex. Cytoarchitectonic features of **LO** are not distinguishable in this Figure.

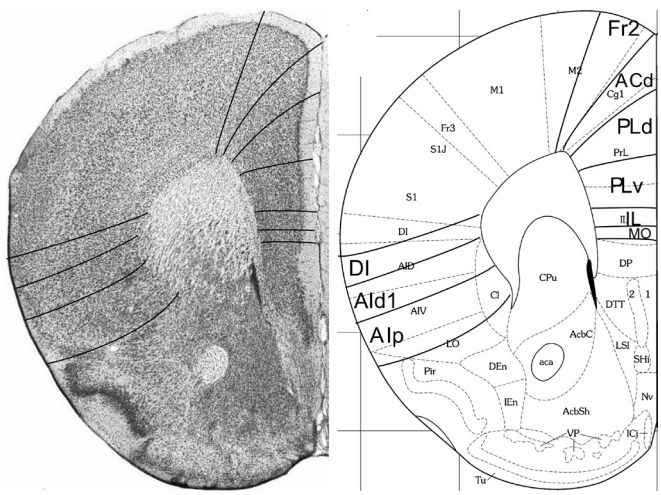

Fig. 6 Implementation of 'Van de Werd et al., 2010' boundaries at Bregma 1.70 mm. *(adapted from Franklin & Paxinos, 2008, The Mouse Brain in Stereotactic Coordinates, Academic Press, Elsevier, N.Y., USA)*

Bregma 1.70 mm (Fig. 6): The major change with the previous figure is the absence of area **AId2** and the presence of the posterior agranular insular area (**AIp**). The area **AIp** is distinguished by the lower cell density in layer III and the small cells of layer V in comparison with **AId1** (see Appendix 1). At this level the atlas maintains the *AID* and *AIV* designations. In the medial prefrontal cortex the ventral boundary of **PLv** doesn't correspond here with the ventral boundary of *PrL*. The ventral boundary of **MO** is roughly the ventral boundary of *IL* as it is in Fig. 5.

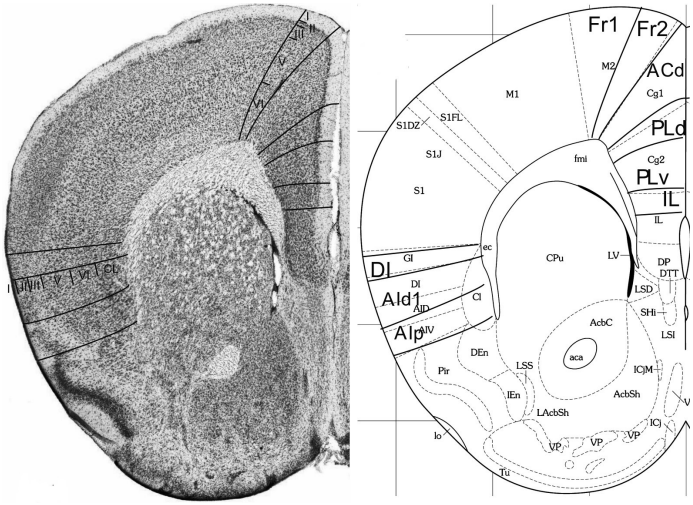

Fig. 7 Implementation of 'Van de Werd et al., 2010' boundaries at Bregma 1.42 mm. *(adapted from Franklin & Paxinos, 2008, The Mouse Brain in Stereotactic Coordinates, Academic Press, Elsevier, N.Y., USA)*

Bregma 1.42 mm (Fig.7): Boundary **Fr2/Fr1** is easily defined in area *M2*, by the typical characteristic differences in layer II, the position of layer V in relation to the pial surface, and the difference in the cellular columns in layers V and VI on both side of the boundary. Area **ACd** is roughly *Cg1*, except the ventral boundary of **ACd** is more dorsal. Given the cytoarchitectonic features described in Appendix 1, the **PLd/PLv** boundary is located in *Cg2*. The *Cg2/IL* boundary corresponds with the **PLv**/**IL** boundary. At this level in the atlas *IL* has a greater extension

more in ventral direction. In the medial PFC we still define the areas **PLd**, **PLv** and **IL** because the features of these areas are more in line with the cytoarchitectonic criteria for these areas than with the criteria for ventral anterior cingulate areas (see Appendix 1). The differences in the lateral prefrontal areas are similar to those described in Fig. 6.

3.1.4. Frontal lobe PFC dorsal to the corpus callosum

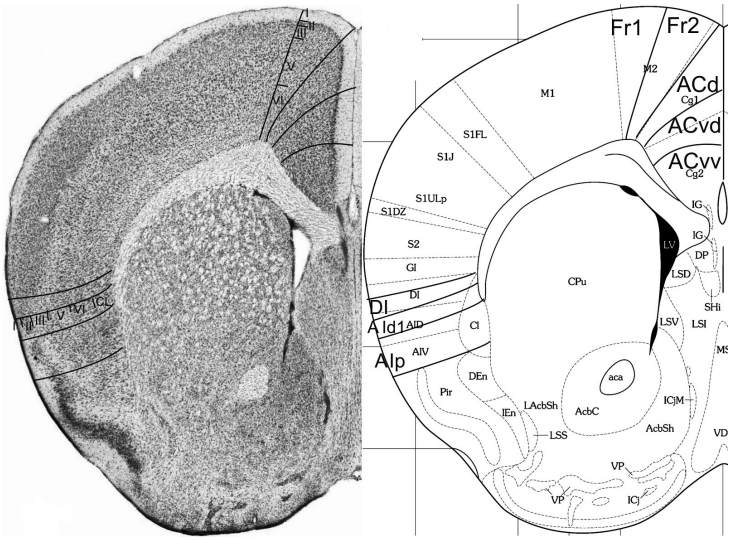

Fig. 8 Implementation of 'Van de Werd et al., 2010' boundaries at Bregma 1.18 mm. *(adapted from Franklin & Paxinos, 2008, The Mouse Brain in Stereotactic Coordinates, Academic Press, Elsevier, N.Y., USA)*

Bregma 1.18 mm (Fig. 8): Boundary **Fr2/Fr1** is defined in *M2*, as in nearly all previous Figures. The characteristics of boundaries **Fr2/Fr1** and **Fr2/ACd** are all present, and typical. The characteristics of boundary **ACd/ACvd** differ from the characteristics of boundary **ACd/PLd** mainly in as far as in **ACvd** layer III is wider and contains less densely packed cells than in **PLd**. The boundary **ACd/ACvd** is mainly characterized by the difference in layer II, which is narrow in **ACd** and shows densely packed cells at the boundary with layer I, but which in **ACvd** is slightly broader

and contains densely packed cells (see also Appendix 1 for other features). This boundary is located in *Cg1*. Boundary **ACvd/ACvv** is characterized on the basis of layers II, III, V and VI (see Appendix 1). On the basis of their typical characteristics, boundary **ACvd/ACvv** is in the dorsal half of *Cg2*. The distinction of **AIp** instead of **AId2** or *AIV* in this figure is based on the clearly separated (sub)layers and the smaller cells of layer V in **AIp** compared with **AId1** or *AID*.

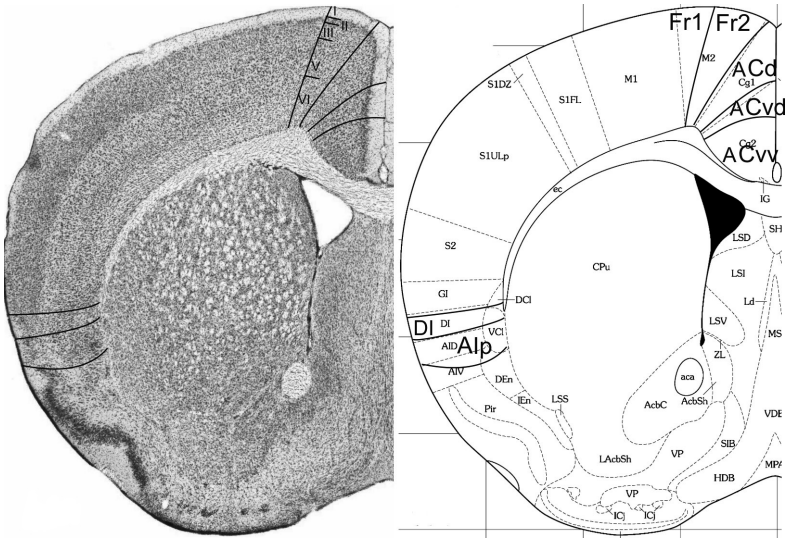

Fig. 9 Implementation of 'Van de Werd et al., 2010' boundaries at Bregma 0.74 mm. *(adapted from Franklin & Paxinos, 2008, The Mouse Brain in Stereotactic Coordinates, Academic Press, Elsevier, N.Y., USA)*

Bregma 0.74 mm (Fig. 9): Boundary **Fr2/Fr1**, located in area *M2*, is mainly defined on the basis of the characteristics of layer V and the cellular columns in layers V and VI. All other boundaries are clearly distinguishable by the characteristics described for the previous Figure. At this level *Cg1* is approximately in the same location as **ACd**. Boundary **ACvd/ACvv** is in the dorsal half of *Cg2*. No **AId1**, as defined in Appendix 1, is detectable at this level.

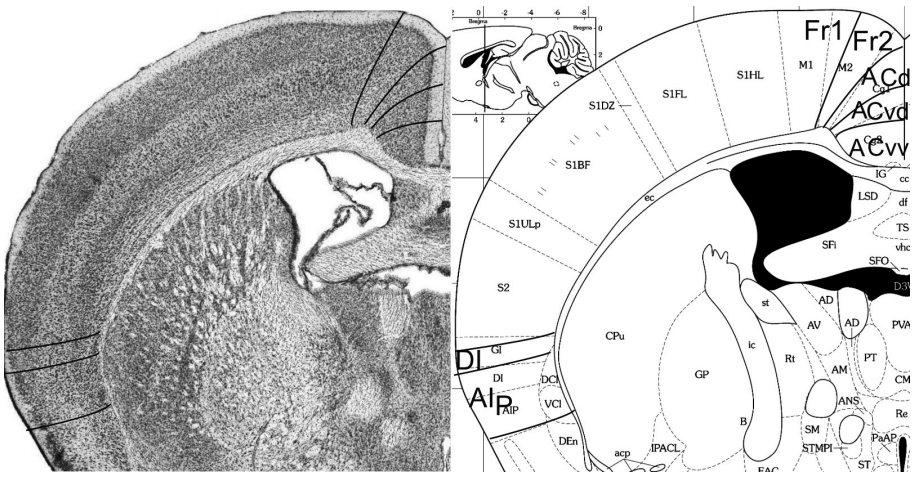

Fig. 10 Implementation of 'Van de Werd et al., 2010' boundaries at Bregma -0.46 mm. *(adapted from Franklin & Paxinos, 2008, The Mouse Brain in Stereotactic Coordinates, Academic Press, Elsevier, N.Y., USA)*

Bregma -0.46 mm (Fig. 10): In the medial PFC, the figure shows denser packing of cells in the **ACv** subareas **ACvd** and **ACvv** than in the areas **Fr2** and **ACd**. The figure is also illustrative for the absence of cellular columns in **ACvd** and **ACvv** and their presence in the dorsal areas **Fr2** and **ACd**. In both **ACvd** and **ACvv** the cells of layer VI are arranged in rows, parallel to the cortical surface, but not in **Fr2** and **ACd**. These four clearly distinguishable areas demonstrate that a more detailed parcellation of the medial PFC is possible than shown in the atlas. At this level the atlas indicates the presence of *posterior agranular insular area, AIP* in the lateral frontal cortex. The distinction and location of **DI** and **AIp** is roughly similar to *GI*, *DI* and *AIP* in the atlas.

Bregma -0.94 mm: The retrosplenial region which includes the agranular retrosplenial area (**RSA**) and the granular retrosplenial area (**RSG**) is immediately caudal to the PFC region. The retrosplenial region is well identifiable by the very typical narrow band of densely packed granular cells in layer II of area **RSG**. **RSA** and **RSG** correspond well with *RSD* and *RSGc*, respectively. This means that the boundary with *M2* is identical here.

3.2. Comparison with Hof et al. (2000)

In their atlas, Hof et al. have indicated the boundaries between cytoarchitectonic areas by arrows positioned at the pial surface. In the original 'image'-files of Nissl sections in Hof et al., curvilinear boundaries have been assessed according to the 'Van de Werd et al.' parcellations. Where cytoarchitectonic characteristics were insufficient, e.g. by artefacts, we had to extrapolate from characteristics visible in the contralateral side, or from an anterior or posterior section.

3.2.1 Frontal pole

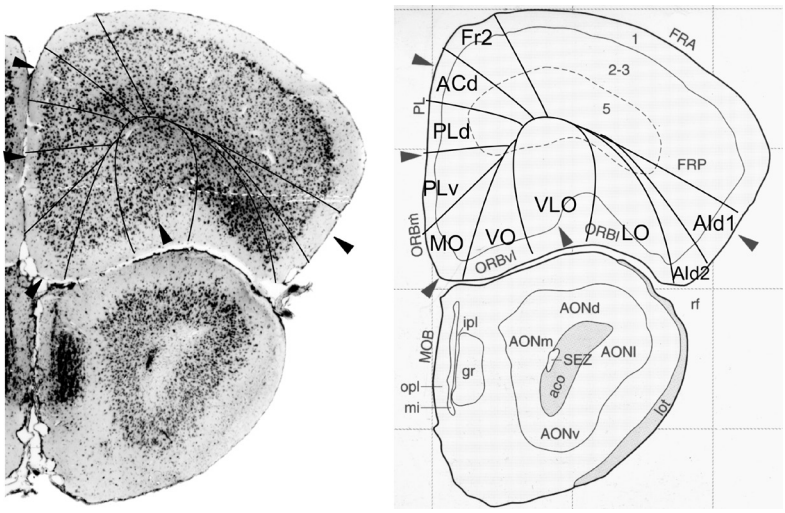

Fig. 11 Implementation of 'Van de Werd et al., 2010' boundaries at Bregma 2.50 mm. *(adapted from Hof et al, 2000, Comparative Cytoarchitectonic Atlas of the C57BL/6 and 129/Sv Mouse Brains, Elsevier, Amsterdam, The Netherlands)*

In Fig. 11, at *Bregma 2.50 mm*, the characteristics of the PFC boundaries are difficult to distinguish. They could only be reliably identified in combination with the aid of extrapolation from the contralateral hemisphere and from the section shown in Fig. 12. Some features are distinguishable even without the need to rely on supplementary information. For example, on the medial side, the widening of layer II in ventral direction is clearly visible,

as is the higher concentration of cells on the boundary between layers I and II in the dorsal half of the medial PFC. In the areas delineated by us as **VO**, **VLO**, **LO** on the ventral side and as **AId1** and **AId2** on the lateral side, mutual differences in the cytoarchitecture are visible that support our parcellation. In the PFC parcellation of the atlas only four areas are recognized of which especially the *orbital cortex, lateral part (ORBl)* shows at least three different cytoarchitectonic structures.

3.2.2 Frontal lobe anterior to the forceps minor

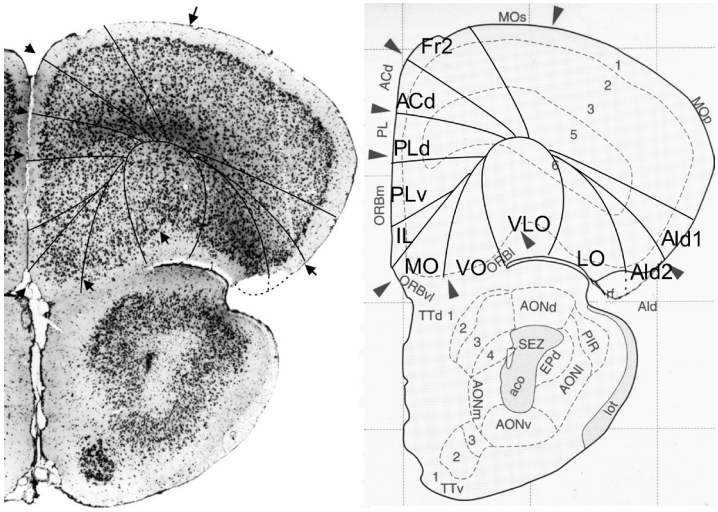

Fig. 12 Implementation of 'Van de Werd et al., 2010' boundaries at Bregma 2.40 mm. *(adapted from Hof et al, 2000, Comparative Cytoarchitectonic Atlas of the C57BL/6 and 129/Sv Mouse Brains, Elsevier, Amsterdam, The Netherlands)*

In Fig. 12, the areas of the PFC are much easier to distinguish than in the previous figure. Thus the smooth aspect of the boundary between layer I and layer II in **Fr2** and the irregular concentration of cells of layer II at the boundary with layer I in **ACd** is now visible. The dorsal and ventral parts of **PL** are distinguishable by the characteristic features in layer II. The area **IL** is estimated between the wide layer II of **PLv** and the wide layer II with densely packed and evenly dispersed cells of **MO**. The ventral

boundaries of **Fr2, ACd, PLd** and **IL,** and the lateral boundaries of **MO** and **AId2** correspond with boundaries in the atlas. The structure of **VO** is quite different from the one in the adjacent areas **MO** and **VLO**. What is remarkable and not easy to explain is that in the atlas the area *ORBl* in Fig. 12 is localized in the medial half of the ventral side of the frontal lobe, whereas in Fig. 11 this area occupies the lateral half of the ventral side of the frontal lobe and the ventral part of the lateral cortex. Architectonically the *dorsal agranular insular area, AId,* in Fig. 12 is not essentially different from area *ORBl* in Fig. 11.

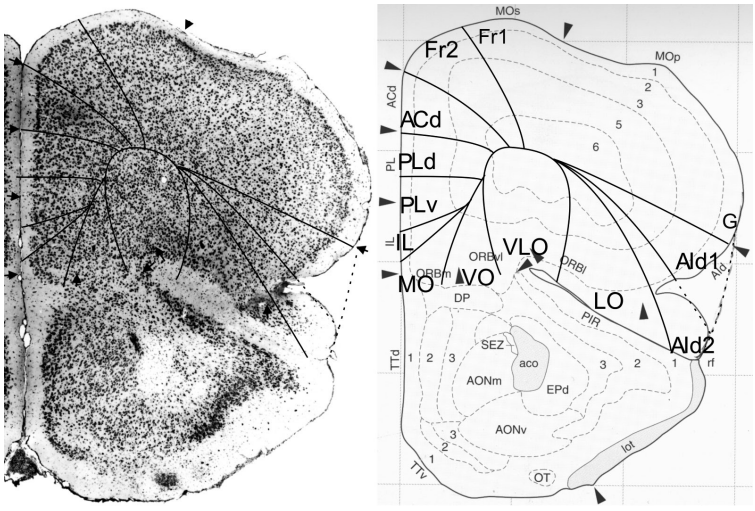

Fig. 13 Implementation of 'Van de Werd et al., 2010' boundaries at Bregma 2.00 mm. *(adapted from Hof et al, 2000, Comparative Cytoarchitectonic Atlas of the C57BL/6 and 129/Sv Mouse Brains, Elsevier, Amsterdam, The Netherlands)*

In Fig. 13 at *Bregma 2.00 mm*, area *ORBl* is again localized in the lateral half of the ventral PFC. The area **IL** is now better recognizable as a homogeneous area. The difference in the aspect of layer II and the different packing of cellular columns in the areas **AId1** and **AId2** is decisive for the recognition of these areas. For the assessment of the boundary **VLO/LO,** the cellular columns in the layers II and III in area **VLO** and the clustering

of cells in layer II of **LO** are decisive. At this level, the ventral boundaries of **Fr2, ACd,** and **IL,** the lateral boundaries of **MO** and **LO,** and the dorsal boundary of **AId1** correspond with boundaries in the atlas.

3.2.3. Frontal lobe anterior to the genu of the corpus callosum

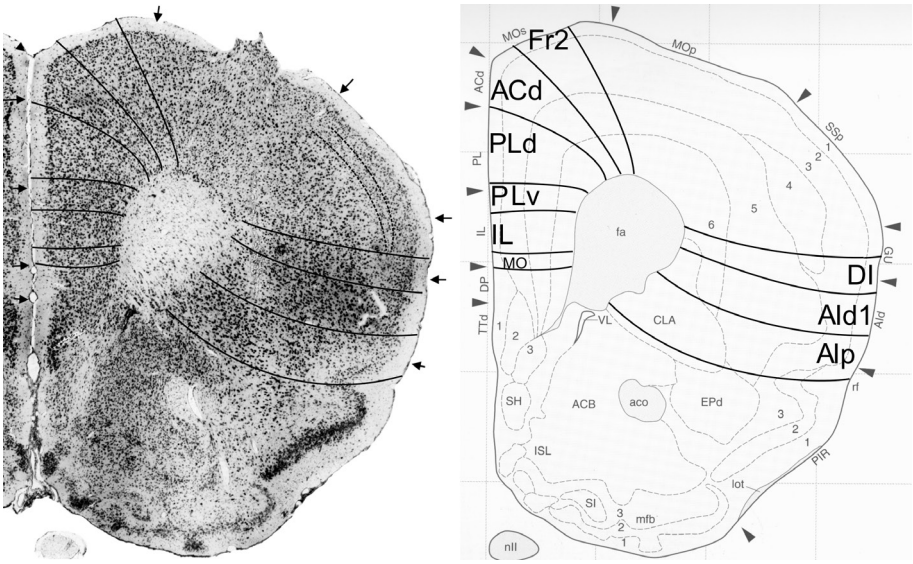

Fig. 14 Implementation of 'Van de Werd et al., 2010' boundaries at Bregma 1.60 mm. *(adapted from Hof et al, 2000, Comparative Cytoarchitectonic Atlas of the C57BL/6 and 129/Sv Mouse Brains, Elsevier, Amsterdam, The Netherlands)*

At *Bregma 1.60 mm* (Fig. 14), in the medial PFC cells are more densely packed in the ventral areas **PLv**, **IL** and **MO** than in the dorsal areas **Fr2**, **ACd** and **PLd**. The characteristics of the medial PFC areas are all clearly visible. In our parcellation more areas are recognized than in the atlas. The ventral boundaries of **ACd,** and **MO** correspond with atlas boundaries. On the lateral side the areas **DI**, **AId1** and posterior agranular insular area (**AIp**) are detected. The area **AId1** is distinguished from **DI** by the cellular columns that are visible in **AId1**, not in **DI**. Identification of **DI** and **AId1** is hampered by an artifact in the deeper cortical layers. The dorsal boundary of **DI** is characterized by the end of the layer IV granular band specified

by interrupted lines in Fig. 14. The area **AIp** is mainly characterized by the cells in layer V which are smaller than in layer V of **AId1**, and by the lower cell density in layer III in **AIp** (see Appendix 1 for other characteristics).

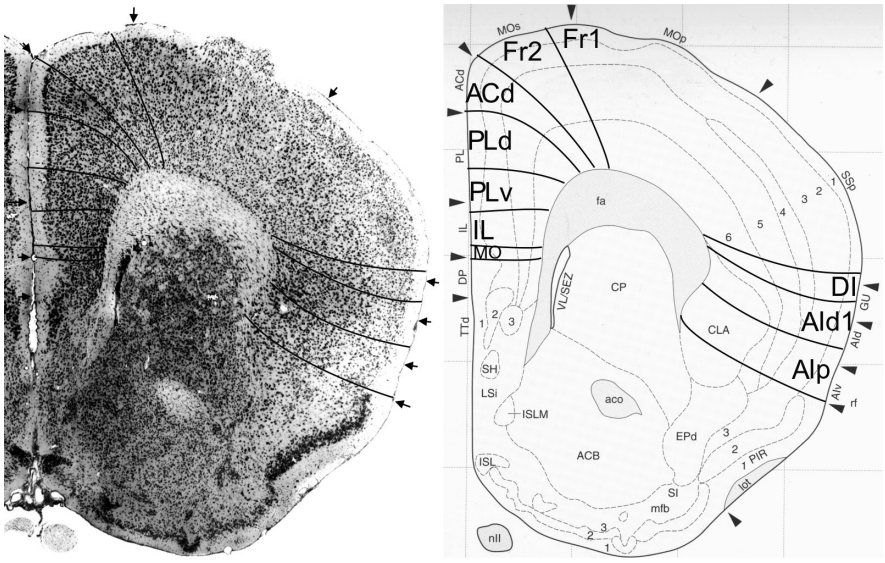

Fig. 15 Implementation of 'Van de Werd et al., 2010' boundaries at Bregma 1.40 mm. *(adapted from Hof et al, 2000, Comparative Cytoarchitectonic Atlas of the C57BL/6 and 129/Sv Mouse Brains, Elsevierin, Amsterdam, The Netherlands)*

At *Bregma 1.40 mm* (Fig.15), all characteristics of the boundaries, described in appendix 1, are distinguishable in the medial PFC. Areas **Fr2** and **ACd** are comparable with *MOs and ACd,* respectively. **PLd** and **PLv** together are approximately in the same position as *PL,* and **IL** and **MO** as *IL*. In the lateral PFC, boundaries **DI/AId1** and **AId1/AIp** are more or less in accordance with the original boundaries in the atlas between the *gustatory cortex* and the *agranular insular cortex, dorsal part* (*GU/AId*) and between *AId* and the *agranular insular cortex,ventral part* (*AId/AIv*), respectively. The ventral boundary of **AIp** equals the ventral boundary of *AIv*.

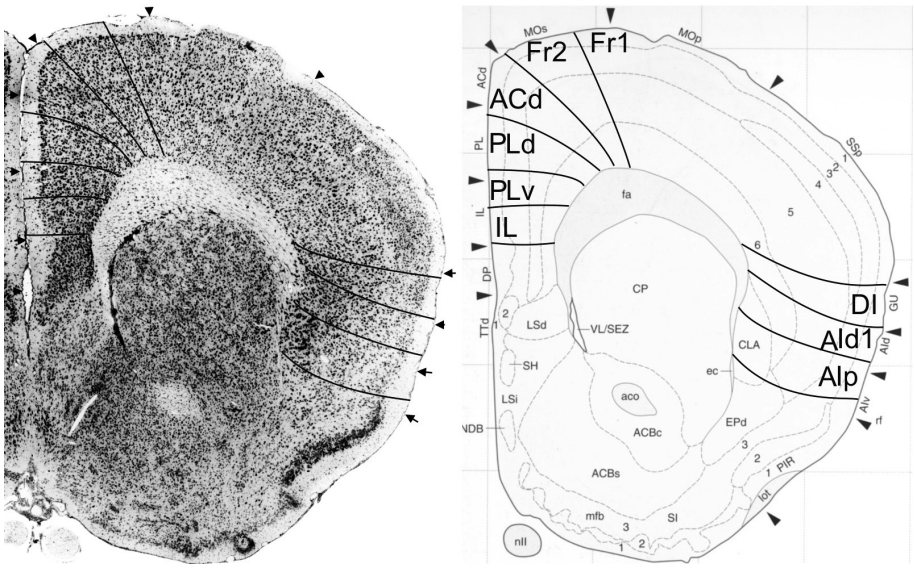

Fig. 16 Implementation of 'Van de Werd et al., 2010' boundaries at Bregma 1.30 mm. *(adapted from Hof et al, 2000, Comparative Cytoarchitectonic Atlas of the C57BL/6 and 129/Sv Mouse Brains, Elsevier, Amsterdam, The Netherlands)*

Bregma 1.30 mm (Fig. 16): In the medial PFC, the medial boundary of **Fr2,** the ventral boundaries of **ACd, PLd and IL** coincide with boundaries in the atlas. On the lateral side of the frontal lobe the areas **DI**, **AId1** and **AIp** approximately correspond with *GU, AId* and *AIv*.

3.2.4. Frontal lobe PFC dorsal to the corpus callosum

Bregma 1.10 mm (Fig. 17): At this level **Fr2** is comparable with the medial half of *MOs* and **ACd** corrresponds with *ACd.* Our distinction of a dorsal and a ventral part in **ACv**, labeled **ACvd** and **ACvv** is supported by the different cytoarchitecture that is visible in these subareas in this Fig. 17. **ACvd** and **ACvv** together coincide with *ACv*. On the lateral side of the frontal lobe, **DI** is more or less comparable to *GU*. At this level we only distinguish **AIp** (see Appendix 1 for defining characteristics). **AIp** is approximately in the same location as *AIv*.

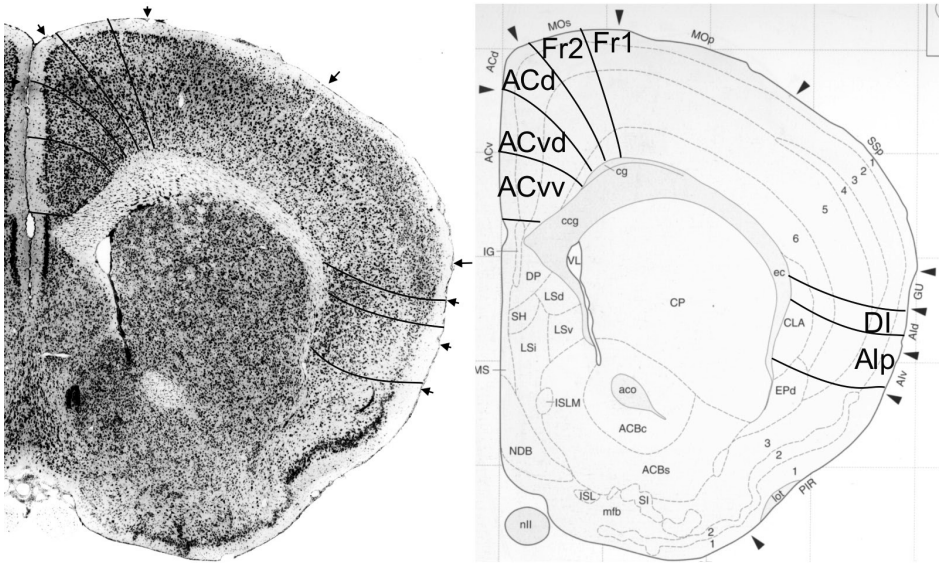

Fig. 17 Implementation of 'Van de Werd et al., 2010' boundaries at Bregma 1.10 mm. *(adapted from Hof et al, 2000, Comparative Cytoarchitectonic Atlas of the C57BL/6 and 129/Sv Mouse Brains, Elsevier, Amsterdam, The Netherlands)*

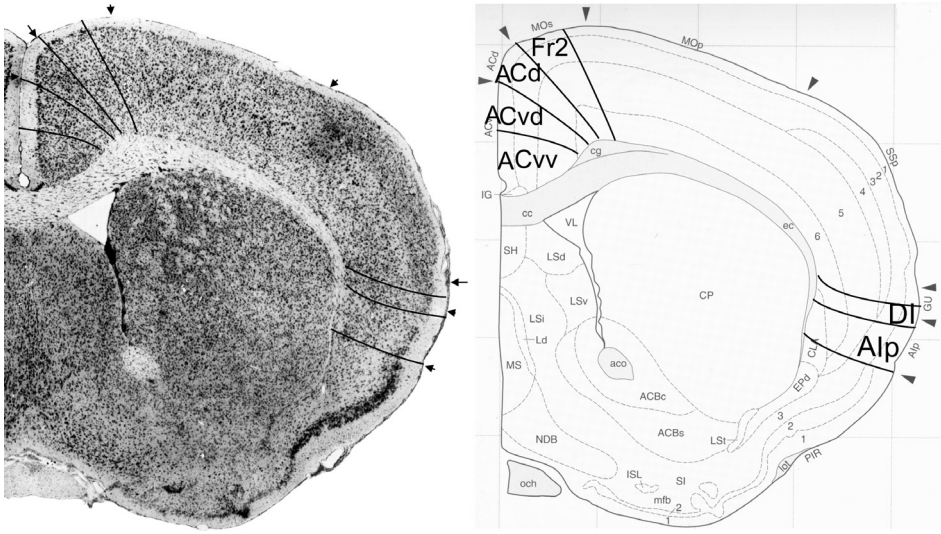

Fig. 18 Implementation of 'Van de Werd et al., 2010' boundaries at Bregma 0.70 mm. *(adapted from Hof et al, 2000, Comparative Cytoarchitectonic Atlas of the C57BL/6 and 129/Sv Mouse Brains, Elsevier, Amsterdam, The Netherlands)*

Bregma 0.70 mm (Fig. 18): At this level the atlas now also identifies the *posterior agranular insular area, AIp* in the lateral PFC, which corresponds with **AIp**. The similarities and differences between the atlas and our distinctions in the medial PFC are as in Fig. 17.

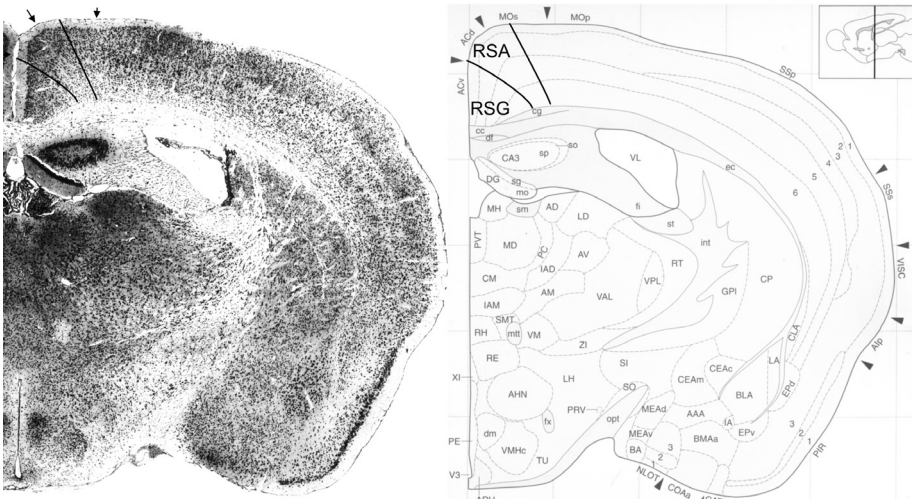

Fig. 19 Implementation of 'Van de Werd et al., 2010' boundaries at Bregma -1.10 mm. *(adapted from Hof et al, 2000, Comparative Cytoarchitectonic Atlas of the C57BL/6 and 129/Sv Mouse Brains, Elsevier, Amsterdam, The Netherlands)*

Bregma -1.10 mm (Fig. 19): In contrast with the atlas we recognize in this figure the retrosplenial region as the typical granular layer II of the granular retrosplenial area (**RSG**) is identifiable at this level. The **RSG** corresponds here with *ACv*. The dorsal boundary of the agranular retrosplenial area, **RSA** is defined in area *MOs*, mainly by the short distance of layer V from the pial surface, due to the absence of layer IV.

3.3. Comparison with Rose (1929)

An important reason to discuss the atlas of Rose is the excellent quality of figures in this study, which makes the distinction between areas generally easy, together with his description of the cytoarchitecture. In the atlas of Rose (1929) boundaries are indicated by arrows placed at the pial surface.

3.3.1. Frontal lobe anterior to forceps minor

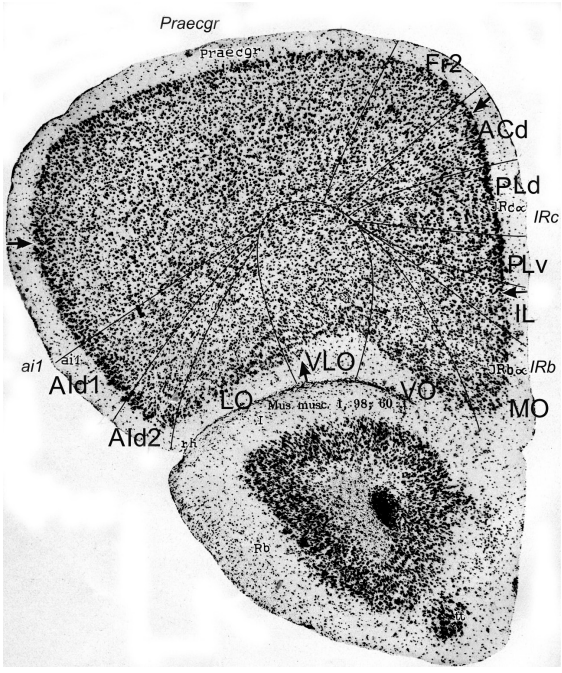

Fig. 20 Implementation of 'Van de Werd et al., 2010' boundaries in section through frontal lobe anterior to forceps minor of Rose (1929)

In Fig. 20 the medial boundary of **Fr2** is approximately comparable with a boundary indicated by Rose, as is the ventral boundary of **PLv.** The agranular **Fr2** is located in the part of the cortex, that is mentioned as granular cortex by Rose. On the lateral cortex, however, we define the extension of the granular and dysgranular cortex more ventrally than Rose does, as we see this boundary just dorsal to the widening of the layer II

in the Rose area *ai 1*. We based the dorsal boundary **AId1** on the cellular columns, the broad, densely packed layer II and the near distance of layer V to the cortical surface. The medial boundary of *ai 1* corresponds with the lateral boundary of **VLO**. Rose defined only one or two ventral PFC areas at this level.

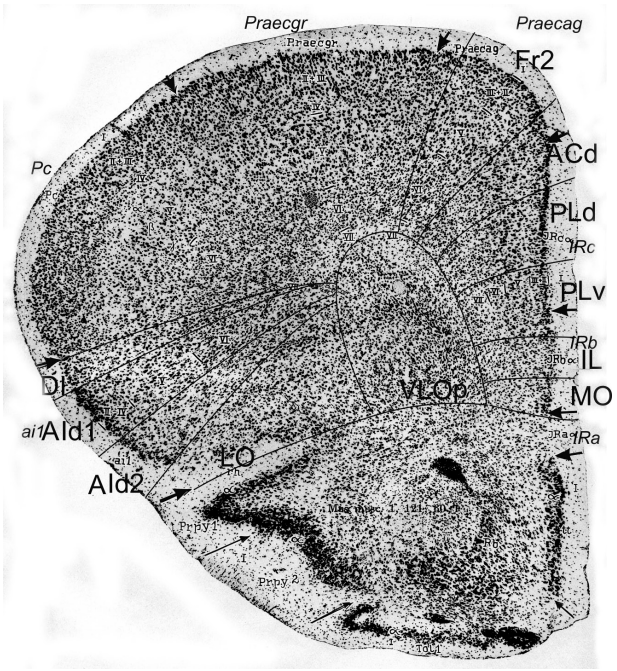

Fig. 21 Implementation of 'Van de Werd et al., 2010' boundaries in section through frontal lobe near forceps minor of Rose (1929)

At the coronal level of Fig. 21, in our parcellation, the extent of the granular cortex is similar to the extent of the granular cortex in the Rose parcellation. The medial PFC areas are well definable on the basis of our criteria. Area **Fr2** is now positioned in the *regio praecentralis agranularis (Praecag),* which area is defined by Rose among others on layer I being narrower than in the adjacent regions, the more dense packing of small cells of layer II at the boundary with layer I, and the gradual transition between the layers III, V and VI. Area **Fr2** is smaller and positioned between

the boundaries of *Praecag.* This is probably caused by a slightly different appreciation of characteristics, as might be our preference for the location of the change in layer V at the lateral boundary of **Fr2** and, at the medial boundary of **Fr2** our choice for the difference in the packing of the cellular columns in delineating boundary **Fr2/ACd**. Areas **ACd**, **PLd**, **PLv, IL** and **MO** are here rather easy to define according to the criteria specified in Appendix 1. T

3.3.2. Frontal lobe anterior to genu of the corpus callosum

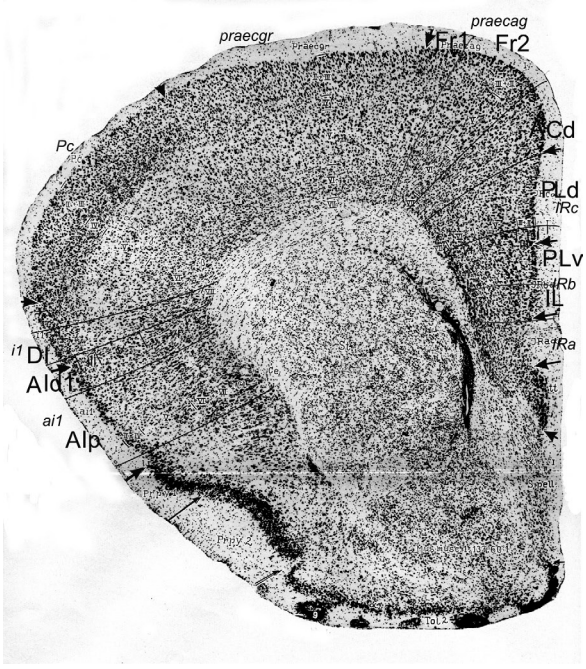

Fig. 22 Implementation of 'Van de Werd et al., 2010' boundaries in section through frontal lobe anterior to genu of the corpus callosum of Rose(1929)

In Fig. 22, the combined areas **ACd** and **Fr2** are approximately comparable with *Praecag*. Also in this Fig.24 **PLd, PLv** and **IL** are easily definable (Appendix 1)**.** On the lateral side of the frontal lobe, the boundary **DI/ AId1** is equal to boundary between *anterior granular insular area* and the

anterior agranular insular area (i 1/ai 1). The ventral boundary of **AIp** is approximately the ventral boundary of *ai 1.* We define **AId1** in the dorsal part of *ai1* (Appendix 1). We agree with Rose that the cells of the claustrum are larger than the cells of the cortical layer VI. Criteria that define equal boundaries in our parcellation and in the parcellation of Rose, show a high degree of correspondence and indicate the value of delineations on the basis of circumscribed criteria of boundaries.

3.3.3. Frontal lobe dorsal to corpus callosum

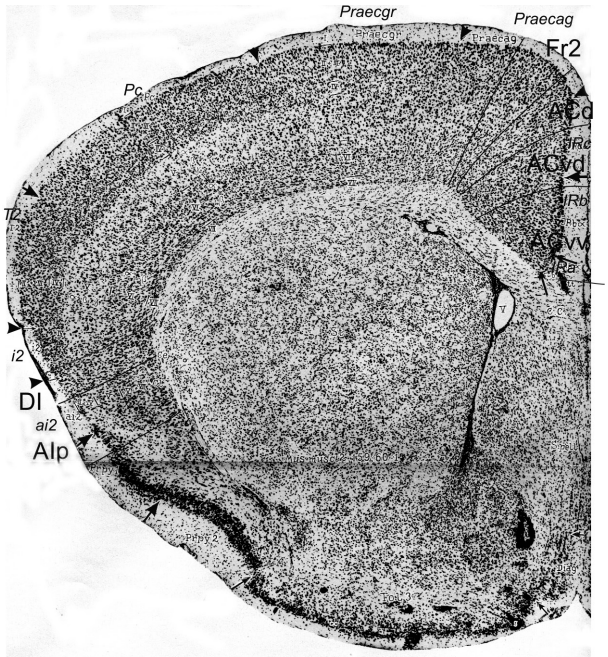

Fig. 23 Implementation of 'Van de Werd et al., 2010' boundaries in section through frontal lobe just caudal to genu of the corpus callosum of Rose (1929)

In Fig. 23, we distinguish, ventrally to area **ACd**, the areas **ACvd** and **ACvv**. The difference in the density of the packing of cells is more gradual between **ACvd** and **ACvv** than between **PLd** and **PLv** in the previous sections. The ventral boundary of **ACvd** is approximately equal to a ventral boundary of Rose. On the lateral side of the frontal lobe we distinguish the

areas **DI** and **AIp** (see Appendix 1) as localized in the Rose area *ai 2*. The cytoarchitecture of **DI** is different from the cytoarchitecture of **AIp**, but in the parcellation of Rose they both are located in area *ai 2*.

3.4. Comparison with other mouse PFC parcellations

Caviness (1975) and Wree et al. (1983) have published studies on the boundaries of mouse cortical areas, including areas of the PFC. In both studies a limited number of photographs are presented which illustrate areas in the prefrontal cortex. In these photographs we have drawn boundaries based on our criteria for delineating the PFC areas.

3.4.1. Caviness (1975)

For the denomination of mouse cortical areas Caviness (1975) has applied a number terminology derived from Brodmann (1909) and Krieg (1946).

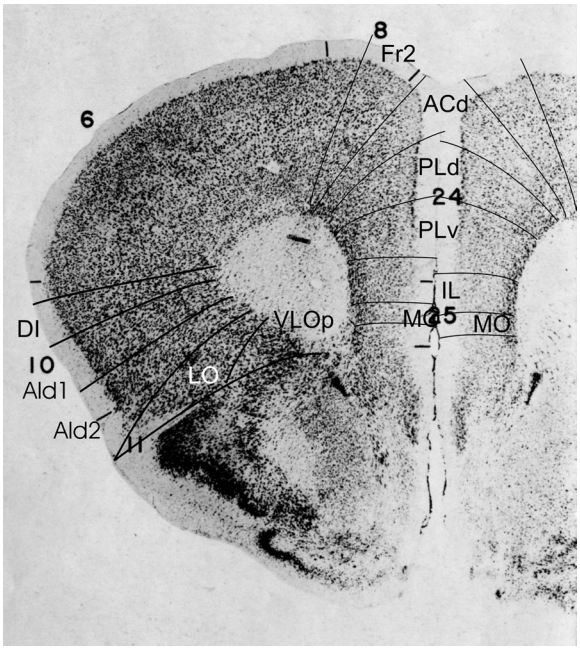

Fig. 24 Implementation of 'Van de Werd et al., 2010' boundaries in section through forceps minor of Caviness (1975)

In Fig. 24, in the medial PFC, it is possible to differentiate the PFC areas **Fr2** and **ACd** mainly on the basis of the packing density of the cellular columns of layers V and VI, and on the cells in **Fr2** which are larger than in **ACd**, rather than on the differences in layer II. Most of area **Fr2** is in *field 8.* In *field 24*, at least three different areas are distinguishable on the basis of the cytoarchitecture. **IL** is partly in *field 24,* and partly in *field 25.* **IL** is recognizable by the homogeneous layers II, III and V. The boundaries of **MO** are estimations because the resolution did not allow to delineate this area with complete reliability. On the lateral side of the frontal lobe, it is difficult to compare our parcellation with the parcellation of Caviness (1975) because in the two *fields 10 and 11,* we distinguish five different areas which show only a very restricted relation with the *fields 10 and 11*.

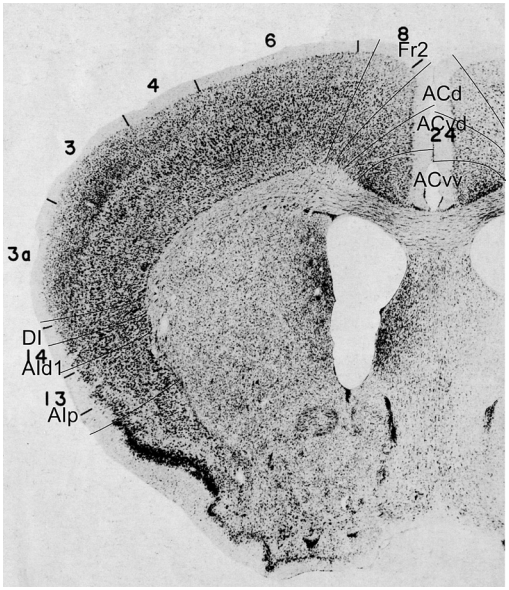

Fig. 25 Implementation of 'Van de Werd et al., 2010' boundaries in section through frontal lobe dorsal to corpus callosum and anterior to hippocampus of Caviness (1975)

In Fig. 25, area **Fr2** largely corresponds with *field 8*. In *field 24* areas **ACd**, **ACvd** and **ACvv** can be distinguished on the basis of the criteria described

in Appendix 1. In *field 14* the areas DI and AId1 are distinguishable. In *field 13* the separation between the cortical layers is characteristic for the identification of area AIp.

3.4.2. Wree et al. (1983)

Wree et al. (1983) compare Nissl stained sections with the images generated by the Grey Level Index (GLI). Boundaries are only presented in the GLI images and indicated by arrow heads.

We have delineated boundaries according to our parcellation system in the Nissl micrograph and subsequently copied them in the GLI image.

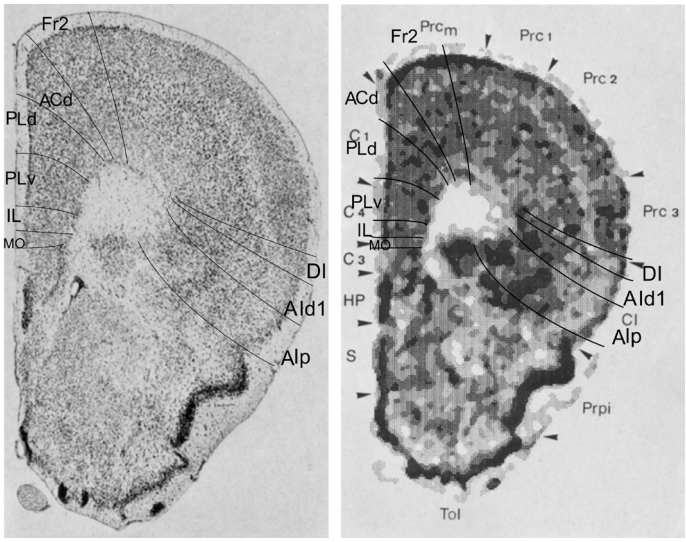

Fig. 26 Implementation of 'Van de Werd et al., 2010' boundaries in section through forceps minor of Wree et al. (1983)

In Fig. 26, the areas of the medial PFC as well as the areas in the lateral PFC are clearly distinguishable in the Nissl micrographs according to the cytoarchitectonic criteria specified in Appendix 1. The areas **PLv**, **IL** and **MO** correspond together to *cingulate area 4 (C4),* the areas **ACd** and **PLv** approximately to the *cingulate area 1 (C1).* Wree et al didn't specify different areas in the lateral PFC, but in this figure the whole *claustrocortex, Cl*, corresponds to **DI, AId1** and **AIp** together.

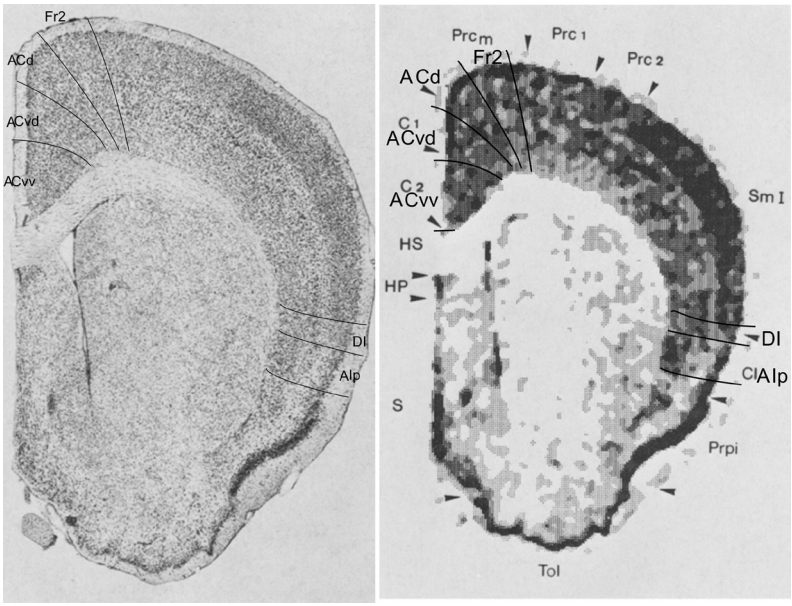

Fig. 27 Implementation of 'Van de Werd et al., 2010' boundaries in section through frontal lobe dorsal to corpus callosum and anterior to hippocampus of Wree et al. (1983)

In Fig. 27, the lateral boundary of **Fr2** is approximately the lateral boundary of the *medial precentral area Prcm*. *Prcm* roughly encompasses both **Fr2** and **ACd**. Boundary **ACd/ACvd** (see Appendix 1) is approximately boundary *Prcm/C1*. Boundary **ACvd/ACvv** (see Appendix 1) is equal to boundary *C1/C2*. Dorsally to the corpus callosum the *cingulate areas 1 and 2* coincide with **ACvd** and **ACvv,** respectively. At this level the whole *claustrocortex, Cl,* in the lateral side of the frontal lobe approximately encompasses **DI** and **AIp**.

3.5. Comparison summarized in Tables

3.5.1. Comparison of presence of boundaries subareas

In Table 1, we have evaluated whether or not the boundaries of the PFC subareas described by Van de Werd et al. (2010) are present in the

publications compared with each other in this review *regardless of* the terminology applied. Due to the fact that we could not always delineate a particular PFC boundary in one of the available micrographs of a publication or atlas, a comparison has not always been possible. We have indicated the areas in the frontal pole anterior to the forceps minor before the symbol '**/**', and the areas caudal to the tip of the forceps minor after the symbol '**/**'.

In the publications of Caviness (1975) and Wree et al. (1983), boundaries are only shown in coronal sections caudal to the forceps minor.

Table 1 indicates that many boundaries show a broad agreement with at least one of the publications reviewed and that a few agree quite well in at least two atlases, i.e. **Fr2**/**ACd**, **ACd**/**PLd**, **ACd**/**ACvd**, and **AId2**/**LO**.

Table 1. Comparison boundaries anterior and posterior to tip of the forceps minor.

Van de Werd et al. (2010)	Franklin & Paxinos (2008)	Hof et al. (2000)	Rose (1929)	Caviness (1975)	Wree et al. (1983)
Fr1/Fr2	$^{+}$–/–	–/~	$^{-}$+/~	/~	/~
Fr2/ACd	$^{-}$+/+	$^{\sim}$+/+	$^{-}$~/~	/+	/~
ACd/PLd	$^{-}$+/+	$^{-}$+/+	–/+	/–	/–
PLd/PLv	$^{+}$–/–	$^{+}$–/~	–/~	/–	/+
PLv/IL	– /+	–/~	–/–	/–	/–
PLv/MO		–/	–/		
IL/MO or IL/DP	–/–	+/+	–/+	/+	/+
MO/DP	~/~	/+	~/+	/~	/+
MO/VO	$^{+}$–/	~/	–/		/
VO/VLO	$^{-}$+/	–/	–/		/
VLO/LO	$^{-}$~/	–/	~/		/
ACd/ACvd	/+$^{\sim}$	/+	/–	/–	/+
ACvd/ACvv	/–$^{+}$	/–	/+	/–	/+
GI/DI	~/~	/~	+/~	/~	/~
GI/AId1 or DI/AId1	+/~	~/+	–/~	/–	/~
AId1/AId2	$^{-}$~/–	–/	–/	/–	
AId2/LO	$^{-}$+ /–	$^{-}$+/	$^{-}$+/	/–	
DI/AIp	/~	/~	/~		/+
AId1/AIp	/~	/+	/~	/~	/+

/ separation region anterior and posterior to tip of forceps minor; + good correspondence of boundary; ~ boundary approximately equal; – no correspondence; symbols in superscript regard the most rostral or most caudal sections of the region under consideration, rostral if in front of the symbol, caudal if after the symbol; *no symbol* boundary not indicated

3.5.2. Comparison of location and extent of subareas

Tables 2 and 3 show the relationship between 'Van de Werd et al. (2010)' areas and areas in the atlases and publications reviewed. The original terminology of the publications is maintained in the Tables. Table 2 considers the frontal lobe anterior to the tip of the Forceps minor, Table 3 the frontal lobe caudal to the tip of the Forceps minor.

In Table 2, the delineations of PFC areas differ widely in the frontal pole. Only just rostral to the forceps minor, correspondence is found for area **ACd** with the comparable area in the Franklin and Paxinos (2008) atlas as well as in the Hof et al. (2000) atlas. Further correspondence is found just rostral to the forceps minor for the Van de Werd et al. (2010) areas **PL** (i.e. **PLd** + **PLv**), **LO** and **VLO** with, respectively, areas *Cg2*, *LO* and *VO* in the atlas of Franklin and Paxinos (2008), and with area *ORBl* in the atlas of Hof et al.(2000). Also **AId1** and **AId2** are together comparable with 'Hof et al' *AId* just rostral to tip forceps minor. The atlas of Franklin and Paxinos (2008) and the atlas of Hof et al. (2000) show a good mutual correspondence between the second motor areas *M2* and *MOs*, and for the medial orbital areas *MO*, at Bregma 2.58 and 2.34 mm, and *ORBm*, at Bregma 2.50 and 2.40 mm, respectively.

Table 2. Comparison of PFC areas anterior to the forceps minor

Van de Werd et al., 2010	Franklin and Paxinos, 2008	Hof et al., 2000	Rose, 1929
Medial			
Fr2	<< PrL → <<< FrA → << M2	<<< FRA → << MOs	<<<Praecgr → < Praecag
ACd	<< PrL → ≈ Cg1	<<< FRA + << PL → ≈ ACd	<<<Praecgr → <<<Praecgr + <<IRc → <<Praecag + << IRc
PLd + PLv	<<PrL + << MO → ≈ PrL	< PL + < ORBm → ≈ PL + << IL	< IRc → < IRc +<< IRb
PLd	<< PrL → < PrL	< PL	<< IRc
PLv	<< MO → < Prl + << MO	< ORBm → << PL + << IL	<<IRc → << IRc + << IRb
IL	<<< MO	<< ORBm → << IL	<< IRb
MO	<< MO	<<ORBm + <<< ORBvl → ≈ ORBvl → ≈ ORBm	<<IRb
Lateral			
AId1 + AId2	< DLO + <<< LO → <AID + < AIV	<<< ORBl + <<< FRA → <<<MOp + << AId → ≈AId	<< ai 1 → << ai 1
AId1	<< DLO + <<< LO → < AID	<<<ORBl + <<<FRA → <<< MOp → <AId	<<< ai 1 → << ai 1
AId2	<<DLO + <<< LO → < AIV	<<<ORBl → <<AId	
Ventral			
LO	<<D LO + < LO → ≈ LO	< ORBl → < AID → < ORBl	<< ai 1
VLO	<< LO + << VO → ≈ VO	<<ORBvl + <<<ORBl → <<ORBl + <<<AId → <<ORBvl + <<ORBl	<<< IRb
VO	< VO → << VO → <<< MO	< ORBvl → <ORBl → <<<ORBm + << ORBvl	<< IRb

<<<: Van de Werd et al. area is a very small part of; <<: VdW-area is a small part of; <: VdW-area is a large part of; ≈: VdW-area is equal or approximately equal to ; → This changes in caudal direction into; +: together with.

Table 3. Comparison of PFC areas posterior to tip forceps minor

	Van de Werd et al., 2010	Franklin and Paxinos, 2008	Hof et al., 2000	Rose, 1929	Caviness, 1975	Wree et al., 1983
R1	*Medial*					
R2	Fr2	< M2	< MOs	<Prcag → ≈ Prcag	≈ 8	< Prcm
R3	ACd	≈ Cg 1	≈ ACd	<<Prcag → <<Prcag + <<IRc → <IRc	<< 24	<Prcm + << C 1
R4	PLd + PLV	≈PrL → ≈PrL + <<IL → ≈Cg2	≈ PL + <<IL→ ≈PL→ ≈PL + <<IL	<IRc + << IRb	< 24	<C 1 + < C 4
R5	PLd	<PrL → <<<Cg1 +<< Cg2	≈ PL → <PL	< IRc	<< 24	< C 1
R6	PLv	<PrL → <<PrL + <<IL → <Cg2	<<IL → <<PL → <<IL	<<< IRc + < IRb	<< 24	< C4
R7	ACvd + ACvv	≈Cg2 + <<Cg1 → ≈ Cg2	≈ ACv	≈ IRb + ≈ IRa + <IRc	< 24	≈C 1 + ≈C2
R8	ACvd	<<Cg1 + <<Cg2 → <<Cg2	< ACv	<IRc	<< 24	≈ C1
R9	ACvv	< Cg2	< ACv	≈ IRb + ≈ IRa	<< 24	≈ C2
R10	IL	<IL → <<IL	<IL	<< IRb	<<<24 + ≈ 25	<< C4
R11	MO	<< IL	<<< IL	<< IRb	<< 25	<<< C4
R12	*Lateral*					
R13	DI	<AId → ≈GI → ≈DI → ≈GI	≈GU → <<AId → <GU	< i 1 → << ai 2	<< 10 → << 14	<<< Cl
R14	AId1 + AId2	<<AID + ≈AIV + <LO		<< ai 1	<< 10 + << 11	
R15	AId1	<<AID + <AIV → ≈DI → <AID	<<AId → <AId + <<GU → ≈AId	<< ai 1	< 10 → < 14	<<Cl
R16	AId2	<< AIV + <LO		<< ai 1		
R17	AIp	<AIV + ≈AIV + <AID → ≈DI + ≈AIP	<<AId → ≈AIv + <<AId → ≈AIp	< ai 1		

<<<: Van de Werd et al. area is a very small part of; <<: VdW-area is a small part of; <: VdW-area is a large part of; ≈: VdW-area is equal or approximately equal to; → This changes in caudal direction into; +: together with.

In Table 3 the relation of areas **Fr2** and **ACd** in Van de Werd et al. (2010) to areas in the atlases of Franklin and Paxinos (2008) and Hof et al. (2000) is very stable, as visible in successive figures. Stable means the relation in position, not necessarily an equal location. Equal location is only found for area **ACd** to areas *Cg1* and *ACd*, respectively. In the atlas of Rose (1929), area *Prcag* correspondents in position and size only most caudally with area **Fr2**. The Van de Werd et al. (2010) areas **ACvd** and **ACvv** together, correspond with area *ACv* in Hof et al. (2000), area **ACvv** corresponds only with Rose' areas *IRb* and *IRa* together. The transition of the prelimbic cortex into the cingulate cortex is at Bregma 1.42 in Franklin and Paxinos (2008), after Bregma 1.30 in Hof et al. (2000) and Van de Werd et al. (2010). The Franklin and Paxinos (2008) area *AIV* at Bregma 1.42 mm is equal to the Hof et al. (2000) area *AIv* at Bregma 1.42 mm. The anterior boundary of the posterior agranular insular area (**AIp**) in Van de Werd et al. (2010) is more rostral to the anterior boundary of this area in Franklin and Paxinos (2008) and Hof et al. (2000). This may be explained by a difference in cytoarchitectonic criteria used. Fluctuation in the position of areas in the ventral side of the frontal lobe is visible in Hof et al. (2000). The Table 2 and Table 3 show that in general no stable relation is found in position and size between ventral areas that are specified in different atlases and publications.

4. Discussion

The aim of this study has been the analysis of the differences that are generally met in the parcellation of the mouse prefrontal cortex (PFC). This is important for the evaluation of subareas of the PFC in relation to results of tracing, morphometric and lesion studies.

The results of this review confirm the existence of a considerable variance in the parcellation of the prefrontal cortex (PFC) in atlases and other publications. The Figures show the varying relation that exists between subareas that have been delineated in accordance with the criteria

summarized in the Appendix, and the subareas specified in the original publications. Anterior to the forceps minor this variance is more obvious (Table 2) than posterior to the forceps minor (Table 3). As extensive series of coronal sections of the prefrontal cortex are only found in the atlases, here we will mainly discuss the difference between the parcellation in the atlases and the 'Van de Werd et al' boundaries. Mutual differences also exist, however, between the atlases themselves, as is visible in the Tables. Some subareas show a mutual low degree of accordance when position and extent of these subareas are considered, e.g., the ventrolateral orbital area (**VLO**) in Van de Werd et al. (2010), ventrolateral orbital area (*ORBvl*) in Hof et al. (2000), and the ventral orbital area (*VO*) in Franklin and Paxinos (2008). In the atlas of Rose (1929) specific areas on the ventral side of the frontal lobe are not even defined. For other subareas, however, as for instance the dorsal anterior cingulate area (**ACd**) in Van de Werd et al. (2010), the dorsal anterior cingulate area (*ACd*) in Hof et al. (2000) and the cingulate area 1 (*Cg1*) in Franklin and Paxinos (2008) there is a very high degree of accordance (see also Tables 1 and 3).

At the other hand, for the position of many boundaries there is a high degree of accordance with the atlases and publications, irrespective of the terminology used. For instance, the boundaries **Fr2**/**ACd**, **ACd**/**PId** and **ACd**/**ACvd** are comparable and correspond with Franklin and Paxinos (2008) and Hof et al. (2000). Boundary **ACvd**/**ACvv** is comparable with a boundary in Rose (1929) and in Wree et al. (1983), see Table 1. Little accordance, however, is found for some other boundaries as for instance **PLv**/**MO** on the medial side of the frontal lobe, **MO**/**VO** on the ventral side of the frontal lobe and **AId1**/**AId2** on the lateral side of the frontal lobe (Table 1).

The differences found in the parcellation of the prefrontal cortex in the atlases and publications, when compared with 'Van de Werd et al.' boundaries, can be explained by (a) difference in the number of subareas, (b) difference in cytoarchitectonic method. (a.) More subareas are defined in e.g. the ventral side of the frontal lobe in our parcellation than in the

atlases and publications reviewed. Thus on the ventral side of the frontal lobe Van de Werd et al. (2010) distinguish both the ventral orbital area (**VO**) and the ventrolateral orbital area (**VLO**), whereas in the atlases of Franklin and Paxinos (2008) and Hof et al. (2000) one single subarea is distinguished instead. The distinction of subareas **VLO** and **VO** on the ventral side of the frontal lobe is corroborated by cytoarchitectonic findings supported by cytochemical characteristics in the mouse (Van de Werd et al., 2010) and supported by the tracing studies in the rat (Groenewegen 1988; Ray and Price 1992; Reep et al. 1996; Schilman et al. 2008). Distinction of a dorsal and a ventral part in the prelimbic area (**PL**) is corroborated by findings in the mouse (Van de Werd et al. 2010, and in one figure of Wree et al, 1983) and in the rat (Heidbreder and Groenewegen 2003; Groenewegen and Uylings 2010; Van de Werd and Uylings 2008). In the mouse we moreover distinguish a dorsal and ventral part in the ventral anterior cingulate area (**ACv**) (Rose, 1929; in one figure in Wree et al., 1983; Van de Werd et al. 2010). In the mouse Franklin and Paxinos (2008) distinguish the dorsolateral orbital area (*DLO*) anterior to the agranular insular areas (*AID*) and (*AIV*). This distinction is not made in the other atlases and publications reviewed in this study. In the rat prefrontal cortex, however, the dorsolateral orbital area (DLO) has been distinguished as an area that is functionally and cytoarchitectonically different from the agranular insular areas (e.g., Ray and Price 1992; Van de Werd et al. 2008; Groenewegen and Uylings 2010; Hoover and Vertes 2011). In the mouse we could not reproducibly define *DLO*. In the rat Van Eden and Uylings (1985), Ray and Price, (1992), and Van de Werd et al. (2008) distinguished the ventral agranular insular area (AIv) on the dorsal bank of the rhinal fissure, but we were unable to distinguish **AIv** on the dorsal bank of the mouse. Given the observed cytoarchitectonic features, we don't consider the mouse area **AId2** to be equivalent with the rat area **AIv** (Van de Werd et al., 2008), but with the rat area **AId2**. (b.) The parcellation methods used are: evaluation of Nissl (Rose 1929), mainly Nissl and AChE (acetylcholinesterase) with a set of cytochemical staining (Franklin and

Paxinos 2008), Nissl and Luxol-Fast-Blue (Hof et al. 2000), Nissl and Fink-Schneider (Caviness 1975), Nissl and GLI (Grey Level Index) (Wree et al. 1983) and Nissl and a set of cytochemical stained sections (Van de Werd et al. 2010). Some of the differences in parcellation can be explained by the use of the additional method next to the Nissl staining. So it is visible in the atlas of Franklin and Paxinos (2008) that for the definition of the prelimbic area (*PrL*), Franklin and Paxinos (2008) rely probably mainly on the data of acetylcholinesterase (AChE) stained sections. This location of *PrL* agrees in general with our cytoarchitectonically defined **PL,** but differs at the "most frontal" sections (Figs. 1 – 2). We have consequently used the same cytoarchitectonic criteria to define **PL**, and therefore also in the most frontal sections. Wree et al. (1983), although presenting Nissl photographs, assessed boundaries mainly on the qualitative evaluation of the GLI data.

In the publications reviewed in this study in general the cytoarchitectonic criteria that have been applied are not fully described. Stereotactic atlases are primarily meant to guide neurophysiological procedures by offering the coordinates to reach a specific subarea of the PFC. In general, they don't present detailed cytoarchitectonic descriptions. On the other hand, in Nissl stained sections, Rose (1929) assessed boundaries upon well described cytoarchitectonic characteristics. Descriptions of the cytoarchitecture of areas in the region of the prefrontal cortex (PFC) were also published by Caviness (1975), De Vries (1912) and Tsuneda (1937). The last two authors, however, illustrate the cytoarchitecture only in isolated area parts, so that the boundaries could not be evaluated. These studies are therefore not further discussed.

The cytoarchitectonic criteria used by Caviness (1975) are more detailed but only few figures are presented while also fewer subareas are distinguished than in the Van de Werd et al. (2010) parcellation.

We only selected Nissl stained photographs which contain PFC areas, for the assessment of boundaries in the prefrontal cortex (PFC) as in general practice the Nissl staining is preferred especially for the PFC boundaries (Van de Werd et al. 2010; Paulussen et al. 2011), and since Nissl staining has proved to be superior to any other staining in visualizing boundaries in general (Van de Werd and Uylings 2008; Van de Werd et al. 2010; Uylings et al. 2010). The Nissl staining is also the staining generally applied in morphometric studies, tracing studies and physiological studies for defining the location of an electrode.

The boundaries we delineated in the original photographs have been constructed on the criteria described in Van de Werd et al. (2010) and summarized in Appendix 1. Overall these criteria could well be discerned in the photographs. In a photograph, however, boundaries are more difficult to assess than when they are examined directly under the microscope. The limitation of the examination in a photograph and the limited number of photographs presented in some publications may be responsible for less precise boundaries in those photographs where the Van de Werd et al. criteria could not be fully applied. Especially in the most rostral cross-sections boundaries had to be partly extrapolated from more caudal cross-sections.

In the atlases and publications reviewed, five different mouse strains have been studied. With the assistance of the criteria described in the Appendix 1 all PFC areas could be defined in these five strains.

Our cytoarchitectonic descriptions focus upon the characteristics at the boundaries (Van Eden and Uylings 1985; Uylings and Van Eden 1990; Van de Werd and Uylings 2008; Van de Werd et al. 2010; Uylings et al. 2010) in contrast to the generally applied procedure of describing cytoarchitectonic characteristics of whole subareas. In addition, we used the requirement that the boundaries are described in such a way that they can be reproducibly positioned by students of PFC. Our cytoarchitectonic parcellation approach of rat PFC appears to better 'fit' the tracing/connectivity studies with the compartments in the thalamic mediodorsal

nucleus, the thalamic midline and intralaminar nuclei, the basal ganglia and amygdala (e.g., Groenewegen 1988; Groenewegen et al. 1990; Schilman et al. 2008; Groenewegen and Uylings 2010; Hoover and Vertes 2011), and functional studies (e.g., Heidbreder and Groenewegen 2003; Dalley et al. 2004). Our parcellation of mouse PFC subareas is in line with the one of rat PFC subareas. Therefore we expect that our cytoarchitectonic criteria and parcellation will be very useful for a more precise localization of electrodes (e.g., Herry and Garcia 2002; Bissonette et al. 2008), microdialysis probes (e.g., Van Dort et al. 2009), receptor binding sites and mRNAs expression (e.g., Amargós-Bosch et al. 2004; Lidow et al. 2003), as well as for anatomical guidance of neuroimaging studies (e.g., Barrett et al. 2003) and tracing neural connections to and from mouse frontal cortical areas (Charbonneau et al. 2012; Parent et al. 2010).

With this review we address a topic which is essential for the understanding of the function of different mouse PFC subareas, and ultimately for the iConnectome (e.g., Hintiryan et al. 2012) and the digital database for multidisciplinary information incorporation, interpretation and reference system (Hawrylycz et al. 2011).

Acknowledgements

This study was supported by Grant RO1 MH61578 (G.Rajkowska (P.I.); H.B.M.U.). We thank Dr. L.J.A. Huisman for correcting the English, and Drs. G. Rajkowska and M.P. Witter and the reviewers of this journal for their constructive critical comments on a previous version of this manuscript.

Conflict of interest: The authors declare that they have no conflict of interest.

References

Amargós-Bosch M, Bortolozzi A, Puig MV, Serrats J, Adell A, Celada P, Toth M, Mengod G, Artigas F (2004) Co-expression and in vivo interaction of serotonin1A and serotonin2A receptors in pyramidal neurons of prefrontal cortex. Cereb Cortex 14:281-299

Bissonette GB, Martins GJ, Franz ThM, Harper ES, Schoenbaum G, Powell EM (2008) Double dissociation of the effects of medial and orbital prefrontal cortical lesions on attentional and affective shifts in mice. J Neurosci 28: 11124-11130

Barrett D, Shumake J, Jones D, Gonzales-Lima F (2003) Metabolic mapping of mouse brain activity after extinction of a conditioned emotional response. J. Neurosci 23:5740-5749

Caviness VS Jr (1975) Architectonic map of neocortex of the normal mouse. J. Comp. Neurol. 164:247-263

Charbonneau V, Laramée ME, Boucher V, Bronchti G, Boire D (2012) Cortical and subcortical projections to primary visual cortex in anophthalmic, enucleated and sighted mice. Eur J Neurosci 36:2949-2963

Dalley JW, Cardinal RN, Robbins TW (2004) Prefrontal executive and cognitive functions in rodents: neural and neurochemical substrates. Neurosci Biobehav Rev 28:771-784

De Vries I (1912) Über die Zytoarchitektonik der groszhirnrinde der Maus und über die Beziehung der einzelnen Zellschichten zum Corpus callosum auf Grund von experimentellen Läsionen. Folia Neuro-Biol 6:289-322

Franklin K, Paxinos G (2008) The Mouse Brain in Stereotactic Coordinates, 3rd edn. Academic Press, Elsevier, San Diego

Groenewegen HJ (1988) Organization of the afferent connections of the mediodorsal thalamic nucleus in the rat, related to the mediodorsal- prefrontal topography. Neuroscience 24:379-431

Groenewegen HJ, Berendse HW, Wolters JG, Lohman AHM (1990) The anatomical relationship of the prefrontal cortex with the striatopallidal system, the thalamus and the amygdala: evidence for a parallel organization. In: Uylings HBM, Van Eden CG, De Bruin JPC, Corner MA, Feenstra MGP (eds) Progress in Brain Research, vol. 85, The Prefrontal Cortex; Its Structure, Function and Pathology. Elsevier Science Publishers, Amsterdam, pp 95-118

Groenewegen HJ, Uylings HBM (2010) Organization of prefrontal-striatal connections. In: Steiner H, Tseng KY (eds) Handbook Basal Ganglia Structure and Function: A Decade of Progress. Academic press, San Diego, pp 353-365

Hawrylycz M, Baldock RA, Burger A, Hashikawa T, Johnson GA, Martone M, Ng L, Lau L, Larsen SD, Nissanov J, Puelles L, Ruffins S, Verbeek F, Zaslavsky I, Boline J (2011) Digital atlasing and standardization in the mouse brain. PLoS Comput Biol 7(2): e1001065, doi: 10.1371/journal.pcbi.1001065

Heidbreder CA, Groenewegen HJ (2003) The medial prefrontal cortex in the rat: evidence for a dorso-ventral distinction based upon functional and anatomical characteristics. Neurosci Biobehav Rev 27:555-579

Herry C, Garcia R (2002) Prefrontal cortex long-term potentiation, but not long-term depression, is associated with the maintenance of extinction of learned fear in mice. J Neurosci 22:577-583

Hintiryan H, Gou L, Zingg B, Yamashita S, Lyden HM, Song MY, Grewal AK, Zhang X, Toga AW, Dong H-W (2012) Comprehensive connectivity of the mouse main olfactory bulb: analysis and online digital atlas. Front Neuroanat doi: 10.3389/fnana.2012.00030

Hoover WB, Vertes RP (2011) Projections of the medial orbital and ventral orbital cortex in the rat. J Comp Neurol 519:3766-3801

Hof PR, Young WG, Bloom FE, Belichenko PV, Celio MR (2000) Comparitive Cytoarchitectonic Atlas of the C57BL/6 and 129/Sv Mouse Brains. Elsevier, Amsterdam

Lidow MS, Koh PO, Arnsten AFT (2003) D1 dopamine receptors in the mouse prefrontal cortex: immunocytochemical and cognitive neuropharmacological analyses. Synapse 47:101–108

Parent MA, Wang L, Su J, Netoff T, Yuan L-L (2010) Identification of the hippocampal input to medial prefrontal cortex in vitro. Cereb Cortex 20:393-403

Paulussen M, Jacobs S, Van Der Gucht E, Hof PR, Arckens L (2011) Cytoarchitecture of the mouse neocortex revealed by the low-molecular-weight neurofilament protein subunit. Brain Struct Funct 216:183-199

Ray JP, Price JL (1992) The organization of the thalamocortical connections of the mediodorsal thalamic nucleus in the rat, related to the ventral forebrain-prefrontal cortex topography. J Comp Neurol 323:167-197

Reep RL, Corwin JV, King V (1996) Neuronal connections of orbital cortex in rats: topography of cortical and thalamic afferents. Exp Brain Res 111:215-232

Rose M (1929) Cytoarchitektonischer Atlas der Groszhirne der Maus. J Psychol Neurol 40:1-51

Schilman EA, Uylings HBM, Galis-de Graaf Y, Joel D, Groenewegen HJ (2008) The orbital cortex in rats topographically projects to central parts of the caudate-putamen complex. Neurosci Lett 432:40-45.

Tsuneda N (1937) Zur Cytoarchitektonik des Neocortex des Mäusegehirns. Okajimas Folia Anat Jpn 15:1-47

Uylings HBM, Van Eden CG (1990) Qualitative and quantitative comparison of the prefrontal cortex in rat and primates, including humans. In: Uylings HBM, Van Eden CG, De Bruin JPC, Corner MA, Feenstra MGP (eds) Progress in Brain Research, vol. 85,The Prefrontal Cortex; Its Structure, Function and Pathology. Elsevier Science Publ. pp 31-62

Uylings HBM, Sanz-Arigita EJ, De Vos K, Pool CW, Evers P, Rajkowska G (2010) 3-D Cytoarchitectonic parcellation of human orbitofrontal cortex, Correlation with postmortem MRI. Psychiat Res: Neuroimag, 183:1- 20

Van De Werd HJJM, Uylings HBM (2008) The rat orbital and agranular insular prefrontal cortical areas: a cytoarchitectonic and chemoarchitectonic study. Brain Struct Funct 212:387-401

Van De Werd HJJM, Rajkowska G, Evers P, Uylings HBM (2010) Cytoarchitectonic and chemoarchitectonic characterization of the prefrontal cortical areas in the mouse. Brain Struct Funct 214:339-353

Van Dort CJ, Baghdoyan HA, Lydic R (2009) Adenosine A(1) and A(2A) receptors in mouse prefrontal cortex modulate acetylcholine release and behavioral arousal. J Neurosci 29:871–881

Van Eden CG, Uylings HBM (1985) Cytoarchitectonic development of the prefrontal cortex in the rat. J Comp Neurol 241:253-267.

Wree A, Zilles K, Schleicher A (1983) A quantitative approach to cytoarchitectonics. VIII. The Areal Pattern of the Cortex of the Albino Mouse. Anat Embryol 166:333-353

Appendix 1

Characteristics

Cytoarchitectonic Characteristics of boundaries (Van de Werd et al., 2010).
1.1. Medial prefrontal subareas anterior to the corpus callosum.

Boundary Fr1/Fr2 (frontal areas 1 and 2)

Columns are seen in both **Fr1** (frontal area 1) and **Fr2** (frontal area 2), but more prominent and more densely packed in **Fr2**. The columns regard the layers V and VI, but in **Fr1** the arrangement of cells in the layer VI might be horizontal instead of columnar.
The size of the cells of the columns is larger in **Fr1** than in **Fr2**.
The layer V rises gradually in **Fr1** to reach its most superficial level at the transition from **Fr1** to **Fr2**. This is due to the progressive loss of cells in the layer IV of **Fr1** as it approaches the agranular **Fr2**.
The layer II shows clefts in **Fr1**, but in **Fr2** the layer II cells join into a smooth, less interrupted layer.

Boundary Fr2/ACd (dorsal anterior cingulate area)

Columns are seen in both areas in the layers V and VI, but they are more densely packed in **ACd** (dorsal anterior cingulate area) than in **Fr2**.
The size of the cells of the columns is smaller in **ACd** than in **Fr2**.
In the layer II of **Fr2** the most superficial cells show a smooth surface with layer I, in **ACd** the cells of the layer II are very much concentrated on its surface, which is irregular.

Boundary ACd/PL (prelimbic area)

Columns are visible in **ACd**, not in **PL**. The layer VI in **ACd** is part of the columnar structure seen in the layers V and VI of that area, but in **PL** the cells of the layer V are not arranged in a recognizable structure and the cells of its layer VI are arranged in horizontal lines, parallel to the pial surface.

The layer V shows columns in **ACd**, but not in **PL**. The cells of the layer V in **PL** are, however, densely packed. The cells of layer V are larger in **PL** than in **ACd**.
The cells of the layer III in **ACd** are less densely packed than the cells of the layer III in **PL**. The layer II in **ACd** is narrow, its cells are concentrated on its surface, in **PL** the layer II is broader and its cells are spread more equally over the whole layer.
Anterior to the fornix minor of the corpus callosum the deeper layers of the PFC are not visible and the features of layer II and less so of layer III will then be the decisive factors in positioning the boundary.

Boundary PLd/PLv (the dorsal and ventral part of PL)

In the prelimbic area **(PL)** we distinguish a dorsal part **PLd** and a ventral part **PLv**.
The layers V and VI are more densely packed in the ventral than in the dorsal part of **PL**. The basic structure of these layers remains, however, the same for the ventral as well as the dorsal part of **PL**.
In both **PLd** and **PLv** the cells of the layer III are less densely packed than in the neighbouring layers. As a result the layer III is lighter in appearance in both parts of **PL**. The layer II is narrower and more densely packed in **PLd** than in **PLv**, where the layer is broader and the cells are less densely packed.

Boundary PL/MO (medial orbital area)

In the most frontal part of the PFC **PL** boundaries **MO**, due to absence of the infralimbic area **(IL)** at that level. The main characteristic of the boundary between **PL** and medial orbital area **(MO)** are the equally dispersed cells of the layer II in **MO** in contrast to the unequal spread of cells in the layer II in **PL**. Layer III separates layer II and V more clearly in **PL** than in **MO**.

Boundary PL/IL (infralimbic area)

The layers II, III and V are well distinguishable from each other in **PL**, but in the infralimbic area (**IL)** they are homogeneous. Some cells of the layer II of **IL** spread into the layer I, but not in **PL** or much less so. The cells in layers II-V are smaller in IL than in PL.

The contrast between the clearly distinguishable layer III in **PL** and the homogeneity of this layer with the neighbouring layers in **IL** is often the easiest sign to determine the boundary between the two areas.

It should be noted that the homogeneity of the layers II, III and V is not always complete in **IL** as sometimes the layer II might be still distinguishable from the other layers. The layer VI shows a horizontal arrangement of its cells in both **PL** and **IL** (infralimbic area).

Boundary IL/MO

The boundary between the infralimbic area **(IL)** and the medial orbital area **(MO)** is characterized mainly by the difference in layer II which is homogeneous with the layers III and V and with spreading of cells of the layer II into layer I in **IL,** while in **MO** layer II has a sharp boundary to the layer III.

The cells of the layer II are very equally dispersed in **MO** but less so in **IL**. The cells of layer II are smaller in IL than in **MO**.

Boundary MO/VO (ventral orbital area)

The boundary between the medial orbital **(MO)** and ventral orbital **(VO)** area is determined mainly by layers I-III. Generally the layer II of the medial orbital area **(MO)** is sharply separated from the layers I and III and the cells in it are rather equally dispersed. In the ventral orbital area **(VO)** the cells of layer II tend to spread into the layer I and the cells in this layer are less densely packed than in **MO**. Also some clustering is present in the layer II in **VO**. The layer III in **MO** may show fine columns, the layer III in **VO** usually does not.

Medial subareas caudally to the genu of the corpus callosum.

Boundary ACd/ACv (ventral anterior cingulate area)

Columns are seen in **ACd** but not in **ACv** (ventral anterior cingulate area). The cells of the layer VI in **ACd** are part of the characteristic columnar structure of that area, but the cells of the layer VI in **ACv** are arranged in horizontal lines.

The cells of the layer V are arranged in columns in **ACd**, but not in **ACv**. The cells of the layer V are densely packed in **ACv**, not in **ACd**.

In both **ACd** and **ACv,** the layer III is easily distinguishable from the neighbouring layers by its light appearance.

The layer II of **ACd** is narrow and its cells are irregularly concentrated on its surface while in **ACv** the layer II is broader and the cells are spread more equally.

Boundary ACvd/ACvv

In **ACv** a dorsal part **(ACvd)** and a ventral part **(ACvv)** are distinguished. In all layers the cells are more densely packed in the ventral than in the dorsal part of **ACv**. In both **ACvd** and **ACvv** the layer III has a light appearance due to the fact that its cells are less densely packed than in the neighbouring layers.

The layer II is narrower and more concentrated in **ACvd** than in the broader layer II of **ACvv**.

Difference between PL and ACv

The contrast of the layer III with the neighbouring layers is clearer in **ACv** than in **PL**. As a consequence the difference between the areas **ACd** and **ACv** is less than between the areas **ACd** and **PL**. The boundary between the layers II and I is sharper in **ACv** than in **PL**.

1.2. Ventral PFC subareas

The ventral areas are known as the ventral orbital **(VO)**, the ventrolateral orbital **(VLO)** and the lateral orbital **(LO)** area and they are distinguished by the following characteristics.

Boundaries VO/VLO/LO

In **VO** the cells of the layer II are not arranged in a recognizable structure. They are unequally spread with some cells spreading into the layer I seeking contact to the retrobulbar region. Also some clustering is present in the layer II in **VO**.

In **VLO** the cells of the layers II and III are arranged in curvilinear vertical columns. **VLO** is usually situated at the ventral notch, the indentation seen on the ventral side of the frontal lobe. The main characteristic of the lateral area **(LO)** is the clustering of cells in its layer II with a sharp transition of that layer to the layer III.

The **VLO** differs from its posterior part**, VLOp**, by the following features. In **VLO** the layers III, V and VI are separated by open zones of low cell density. In the posterior part of **VLO**, distinguished as **VLOp**, however, all layers are more homogeneous.

1.3. Lateral PFC subareas

Boundary of the granular (G) or dysgranular insular cortex (DI) with the dorsal agranular insular area 1 (AId1)

In the frontal part of the PFC the dorsal agranular insular area 1 **(AId1)** boundaries the granular cortex (**G**), but in the caudal part of the PFC **AId1** boundaries the dysgranular cortex **(DI)**.

Columns are seen very clearly in the layers V and VI in **AId1,** not at all or much less impressive and less closely packed in **G** or **DI**.

The cells of layer V are smaller in **AId1** than in **G** or **DI**.

The layers II, III and IV are homogeneous in **DI**, but in **AId1** the layer IV is absent and the layers II and III are well distinguishable from each other.

The cells of the layer III are less densely packed in **AId1** than in **G** or **DI**.

Boundary AId1/AId2 (dorsal agranular insular area 2)

Columns are seen in both areas but they are more densely packed in **AId2** than in **AId1**.

The cells of the layer V are smaller in **AId2** than in **AId1**.

The cells of the layer III are less densely packed in **AId2** than in **AId1**.

The layer II is broad in both areas. In **AId1** layer II cells are densely packed, but in **AId2** the layer II is broken by clefts, its cells partake in the columnar structure of the area and some cells spread into the layer I.

Boundary AId1/AIp (posterior agranular insular area)

In the posterior agranular insular area (**AIp**), the cortical layers and the claustrum are well separated from each other. If the cell-sparse zones between the layers are included as sublayers, 8 or more (sub)layers can be distinguished. In **AId1** the layers are contingent and a columnar arrangement of the cells of the layers V and VI is visible. The cells of layer V of **AIp** are smaller than the cells of layer V in **AId1**.

Boundary AId2/LO

Columns are seen in the layers VI, V and II in **AId2** but not in **LO**. Layer I is narrow in **LO**, broad in **AId2**. The layer II in **AId2** is broad and cells spread to layer I. In **LO** the layer II shows marked clustering of cells.

Appendix 2

Abbreviations in the Franklin and Paxinos atlas (2008)

AI	agranular insular cortex
AID	agranular insular cortex, dorsal part
AIP	agranular insular cortex, posterior part
AIV	agranular insular cortex, ventral part
Cg1	cingulate cortex, area 1
Cg2	cingulate cortex, area 2
Cl	claustrum
DI	dysgranular insular cortex
DLO	dorsolateral orbital cortyex
DP	dorsal peduncular cortex
fmi	forceps minor of the corpus callosum
Fr3	frontal cortex, area 3
FrA	frontal association cortex
GI	granular insular cortex
IL	infralimbic cortex
LO	lateral orbital cortex
M2	secondary motor cortex
MO	medial orbital cortex
PrL	prelimbic cortex
RSD	retrosplenial dysgranular cortex
RSG	retrosplenial granular cortex
VO	ventral orbital cortex

R1
R2
R3
R4
R5
R6
R7
R8
R9
R10
R11
R12
R13
R14
R15
R16
R17
R18
R19
R20
R21
R22
R23
R24
R25
R26
R27
R28
R29
R30
R31
R32
R33
R34

Abbreviations in the Hof et al. atlas

ACd	anterior cingulate cortex, dorsal part
ACv	anterior cingulate cortex, ventral part
AId	agranular insular cortex, dorsal part
AIp	agranular insular cortex, posterior part
AIv	agranular insular cortex, ventral part
CLA	claustrum
DP	dorsal peduncular area
fa	corpus callosum, anterior forceps
FRA	frontal association area
FRP	frontal pole
GU	gustatory cortex
IG	indusium griseum
IL	infralimbic area
MOs	secondary motor cortex
ORBl	orbital cortex, lateral part
ORBm	orbital cortex, medial part
ORBvl	orbital cortex, ventrolateral part
PL	prelimbic area
rf	rhinal fissure
TTd	tenia tecta, dorsal part

Abbreviations in the Rose atlas

ai 1	area insularis agranularis anterior
ai 2	area insularis agranularis posterior
i 1	area insularis granularis anterior
i 2	area insularis granularis posterior
IRa α	area infraradiata ventralis anterior
IRb α	area infraradiata intermedia anterior
IRc α	area infraradiata dorsalis anterior
IRa β	area infraradiata ventralis posterior
IRb β	area infraradiata intermedia posterior
IRc β	area infraradiata dorsalis posterior
Praecag	regio praecentralis agranularis
Praecgr	regio praecentralis granularis

Abbreviations in the Wree et al. study

C 1; 2; 3; 4	area cingularis 1; 2; 3; 4
Cl	claustrocortex
Prc_m	area praecentralis medialis